Working Fluid Data Mining for Energy Harvesting

by

Natchanon Ornsila

A Report Submitted in Partial Fulfillment of the Requirements
for the Degree of Bachelor of Engineering (Petrochemical Engineering)
Department of Chemical Engineering, School of Engineering,
King Mongkut's Institute of Technology Ladkrabang
Academic Yea 2020

การทำเหมืองข้อมูลสำหรับคัดเลือกของไหลภายในระบบเก็บเกี่ยวพลังงาน

โดย

ณัฐชนน อ่อนศิลา

ปริญญานิพนธ์นี้เป็นส่วนหนึ่งของการศึกษาตามหลักสูตร
วิศวกรรมศาสตรบัณฑิต สาขาวิชาวิศวกรรมปิโตรเคมี
ภาควิชาวิศวกรรมเคมี คณะวิศวกรรมศาสตร์
สถาบันเทคโนโลยีพระจอมเกล้าเจ้าคุณทหารลาดกระบัง
ปีการศึกษา 2563

Title	Working Fluid Data Mining for Energy Harvesting
By	Natchanon Ornsila
Field of Study	Petrochemical Engineering
Advisor	Asst.Prof.Dr. Surat Areerat

Accepted by the Faculty of Engineering, King Mongkut's Institute of Technology Ladkrabang in Partial Fulfillment of the Requirements for the Degree of Bachelor of Engineering (Petrochemical Engineering).

Thesis Committee

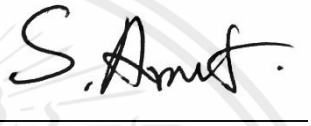

Chairman

(Asst. Prof. Dr. Surat Areerat)

Committee

(Asst. Prof. Dr. Tanawan Pinnarat)

Committee

(Asst. Prof. Dr. Nattapol Lerkkasemsan)

Title	Working Fluid Data Mining for Energy Harvesting
By	Natchanon Ornsila
Advisor	Asst.Prof.Dr. Surat Areerat
Field of Study	Petrochemical Engineering
Affiliation	Department of Chemical Engineering, Faculty of Engineering, King Mongkut's Institute of Technology Ladkrabang

Abstract

The working fluids are interested because are applied in many engineering applications particularly harvesting energy systems. This project explored 1,057 azeotropic binary mixtures from 11,088 binary mixtures which are normal boiling temperatures lower than or equal to the water and calculable by UNIFAC.

The overall process included 3 parts which were data cleaning, data-generating, and data mining. data cleaning was the observation, filter, and structuring of raw data. Data generating was mixture creating, azeotropic mixture finding, mine construction. The construction includes 3 characters of working fluid which consist of primary properties, secondary properties, and safety. The primary properties mean that correlation properties of working fluid which affect to the system. The secondary properties are calculated by primary properties. NFPA diamond was used to consider safety. Some missing properties were fulfilled by group contribution method. Lastly data mining, K-mean clustering is unsupervised machine learning which is applied to grouping similar data.

From the result of data mining, the number of cluster primary properties, secondary properties, and safety are 6, 4, and 6 clusters respectively. For safety, cluster 4 and 5 are possible to do the experiment due to safer clusters than others. For secondary properties, the mixtures in cluster 0 are clustered by primary properties as cluster 0, 1 and, 4 which have R-114 with n-butane (P_{az} = 5.19 bar, $x_{az,1}$=0.57), acetone with R-123a (P_{az} = 2.08 bar, $x_{az,1}$=0.01), and ethanol with R-11(P_{az} = 2.35 bar, $x_{az,1}$=0.02) as the candidates respectively. Cluster 1 has a character of primary properties as cluster 3 which has R-12 with R-218 as a represent mixture (P_{az} = 17.00 bar, $x_{az,1}$=0.25). For cluster 2, primary properties include cluster 1, 2, and 3. Represent mixtures are R-C318 with cis2-butene (P_{az} = 8.26 bar, $x_{az,1}$=0.58), cyclobutane with R-3-1-10 (P_{az} = 6.06 bar,

$x_{az,1}$=0.35), and R-152a with R-134a (P_{az} = 13.48 bar, $x_{az,1}$=0.33) respectively. Cluster 3 of secondary properties has cluster 4 and 5 which represent mixtures is R-21 with cyclobutane (P_{az} = 3.98 bar, $x_{az,1}$=0.90) and R-30 with cyclopentane (P_{az} = 1.49 bar, $x_{az,1}$=0.80). These compounds can be used to design experiment because each mixture has clearly different characters from data mining.

In conclusion, Data mining can assist to decide working fluid selection and design experiments. The group contribution method is another important which helps to mine construction. In the future, data mining for ternary or more mixture is quite interested due to if binary mixtures are friendly environment, will be unsafe.

Keywords: data mining, working fluid, energy harvesting, thermosyphon, group contribution method, and machine learning

เรื่อง	การทำเหมืองข้อมูลสำหรับคัดเลือกของไหลภายในระบบเก็บเกี่ยวพลังงาน
โดย	ณัฐชนน อ่อนศิลา
อาจารย์ที่ปรึกษา	ผศ.ดร.สุรัตน์ อารีรัตน์
สาขาวิชา	วิศวกรรมวิชาปิโตรเคมี
สังกัด	ภาควิชาวิศวกรรมเคมี คณะวิศวกรรมศาสตร์ สถาบันเทคโนโลยีพระจอมเกล้าเจ้าคุณทหารลาดกระบัง

บทคัดย่อ

ข้อมูลที่เกี่ยวกับของไหลทำงานค่อนข้างน่าสนใจ เนื่องด้วยมีการใช้ประโยชน์มากมายในทางวิศกรรมโดยเฉพาะระบบเก็บเกี่ยวพลังงาน โครงการนี้สำรวจคู่สารอะซีโอโทรป 1,057 คู่สาร จาก 11,088 คู่สาร ที่จุดเดือดปกติต่ำกว่าหรือเท่ากับน้ำ ในฐานข้อมูลและสามารถคำนวนด้วย UNIFAC ได้

โดยภาพรวมแล้วประกอบด้วย 3 กระบวนการได้แก่ การทำความสะอาดข้อมูล การสร้างข้อมูล และการทำเหมืองข้อมูล โดยที่การทำความสะอาดข้อมูลนั้นเป็นการสำรวจ คัดกรอง และจัดการโครงสร้างข้อมูลดิบ ในส่วนของการสร้างข้อมูลนั้นเป็นการสร้างข้อมูลของคู่สารผสม การคำนวนหาอะซิโอโทรป และรวมไปถึงการสร้างเหมืองข้อมูล ซึ่งโครงสร้างข้อมูลที่พิจารณาแบ่งได้ 3 ลักษณะ ได้แก่ คุณสมบัติหลัก คุณสมบัติรอง และ ความปลอดภัย โดยคุณสมบัติหลักหมายถึงคุณสมบัติของของไหลที่มีผลต่อระบบต่างๆ สำหรับคุณสมบัติรองเป็นตัวแปรที่คำนวนมาจากคุณสมบัติหลัก และ NFPA 704 ถูกใช้ในการพิจารณาความปลอดภัยของสาร ซึ่งบางสารที่ขาดข้อมูลจะได้รับการเติมเต็มด้วย group contribution method และท้ายสุด ทำเหมืองข้อมูลโดยใช้ K-mean clustering ซึ่งเป็นวิธีการเรียนรู้ของเครื่องในการจับกลุ่มของข้อมูล

จากผลของการทำเหมืองข้อมูลสามารถแบ่งกลุ่มได้ 6, 4, 6 กลุ่มสำหรับ คุณสมบัติหลัก คุณสมบัติรอง และ ความปลอดภัยตามลำดับ ในการเลือกของไหลทำงาน กลุ่ม 4 และ 5 ของการจับกลุ่มตามความปลอดภัยมีความเป็นไปได้ที่จะทำการทดลองเนื่องด้วยปลอยภัยกว่ากลุ่มอื่นๆ ดังนั้นการจับกลุ่มโดยใช้คุณสมบัติรองและคุณสมบัติหลักจะเหลือดังต่อไปนี้ ในกลุ่มที่ 0 ของคุณสมบัติรองจะประกอบด้วยสารที่อยู่ในกลุ่ม 0, 1, และ 4 ของคุณสมบัติหลักซึ่งสารผสมมีตัวแทนดังนี้ R-114 กับ บิวเทน (P_{az} = 5.19 bar, x_{az},1=0.57) อะซิโตน กับ R-123a (P_{az} = 2.08 bar, x_{az},1=0.01) และ เอทานอล กับ R-11 (P_{az} = 2.35 bar, x_{az},1=0.02) ตามลำดับ สำหรับ กลุ่มที่ 1 ของคุณสมบัติรองมีลักษณะของสารเป็นกลุ่มที่ 3 ในคุณสมบัติหลัก ซึ่งมีตัวแทนเป็น R-12 กับ R-218 (P_{az} = 17.00 bar, x_{az},1=0.25) ในกลุ่มที่ 2 ของคุณสมบัติรอง ประกอบด้วย 3 กลุ่มของคุณสบัติหลัก ได้แก่ กลุ่มที่ 1 มี

R-C318 กับ บิวทีน (P_{az} = 8.26 bar, x_{az},1=0.58), กลุ่มที่ 2 มี ไซโครบิวเทน กับ R-3-1-10 (P_{az} = 6.06 bar, x_{az},1=0.35), และ กลุ่มที่ 3 มี R-152a และ R-134a (P_{az} = 13.48 bar, x_{az},1=0.33) เป็นตัวแทน และท้ายสุดกลุ่มคุณสมบัติรองที่ 3 ประกอบด้วย กลุ่มที่ 4 และ 5 ของคุณสมบัติหลัก ซึ่งสามารถใช้ R-21 กับ ไซโครบิวเทน (P_{az} = 3.98 bar, x_{az},1=0.90) และ R-30 กับ ไซโครเพนเทน (P_{az} = 1.49 bar, x_{az},1=0.80) เป็นตัวแทนตามลำดับ ซึ่งคู่สารต่างๆเหล่านี้สามารถใช้ในการออกแบบการทดลองในอนาคตเพื่อศึกษาผลกระทบของของไหลต่อระบบเนื่องด้วยลักษณะที่แตกต่างกันอย่างชัดเจนจากการทำเหมืองข้อมูล

โดยสรุปจะเห็นได้ว่าการทำเหมืองข้อมูลช่วยในการเลือกของไหลทำงานและการออกแบบการทดลองได้ และที่ขาดไม่ได้คือ group contribution method ที่ช่วยเสริมข้อมูลที่หายไป และในอนาคตการทำเหมืองกับสารผสมสามสารค่อนข้างน่าสนใจซึ่งคาดว่ามีความเป็นมิตรต่อสิ่งแวดล้อมและปลอดภัยกว่าสองสาร

คำสำคัญ: เหมืองข้อมูล ของไหลทำงาน เก็บเกี่ยวพลังงาน เทอร์โมไซฟอน group contribution method และ การเรียนรู้ของเครื่อง

Acknowledgements

I would like to express my sincere thanks to my advisor Asst.Prof.Dr. Surat Areerat who provide me an opportunity and believe in me to undertake this project. And then thank you for various support either consultation, knowledge, experience, tool, and pace of mind.

And indispensable, whether it be database and tool for calculation as ProPred in ProCAPE. Hence, thank PSE for Speed Company Limited for ProCAPE program.

I would also like to thank the Department of Chemical Engineer, King Mongkut's Institute of Technology Lardkrabang for various paper research accessing, all opportunity, and various experience.

Finally, I most gratefully all professors and staff in the faculty for providing knowledge, experience, comfort, and security in the meantime of bachelor's degree.

Natchanon Ornsila

Table of Contents

Lis of Figure

Page

List of Tables

Page

Appendix

NOMENCLATURE

Ar	Archimedes number $(gd^3/\nu_l^2)^2(1-\rho_v/\rho_l)$
a	Interaction parameter
Bo	Bond number
C_p	Heat capacity
D	Data value
d	Inner dimeter
Fr	Froude number $(q/\rho_l h_{fg})[\rho_l/dg(\rho_l-\rho_v)]$
g	gravitational acceleration
h	Heat transfer coefficient
h_{fg}	Laten heat of vaporization
Ja	Jakob number
k	Thermal conductivity
L	Length
L_c	Characteristic length
m	Mass flow
n	Number of databases
P	Pressure
Pr	Prandtl number $(\mu C_p/k)$
Q	Heat transfer rate
q	Heat flux
R	Gas constant
Ra	Rayleigh number $(\Delta \rho L_c^3 g \rho C_p)/\mu k$
Re	Reynolds number
S	Specific entropy
T	Temperature
Tr	Residual temperature
X	dimensionless pool parameter
x	Liquid composition
y	Vapor composition

Greek symbol

γ	Activity coefficient
μ	Dynamic viscosity
ν	Kinetic viscosity (μ/ρ)
ρ	Density
σ	Surface tension
Ψ	Mixing coefficient

Subscripts

az	Azeotrop
b	Bubble
c	Condenser
cal	Calculation
cen	Centroid
cri	Critical
e	Evaporator
f	Liquid film
i	identified compound
ig	Ideal gas
l	Liquid
max	Maximum
min	Minimum
NB	Nucleate boiling
nust	Nusselt
prop	Property
s	Surface condition
sat	Saturated condition
TPC	Tow phase convection

CHAPTER I

INTRODUCTION

1.1 Background

Data is the new oil. Data influence with many sectors which chemical engineer is not excepted. Currently, data has been generating huge volumes and faster in the future, which more enough to take advantage but difficult to manage. So, the process for data extracting from raw data is necessary which is called “Data Mining”. Data Mining in a simplified definition is exploring and studying data to understand in patterns and structures of data[1]. This project wishes to apply the process of data mining into field of engineer.

The working fluid is important in many engineer applications whether it be power generation, refrigeration, or heating applications. In this time, working fluid is developed from various fluids. Therefore, data mining is used to survey the character of the fluids to select candidates as working fluids for future experiments. Data mining is a helpful method which given performance and economical experiment. In terms of working fluid selection, an application should be a specific system due to each system has different suitable working fluids. Thus, energy harvesting is an interesting choice at the present. Since, energy has been an important thing to drive the world since the past, present, and more important role in the future, which consistent with Figure 1-1. The figure shows a clearly increasing trend in energy consumption. Also, the most primary energy consumption comes from gas, oil, and coal which are difficult to renewable. Therefore, reducing the consumption of these energy sources and responding to increasing energy demand is interesting in the current. Hence, developing energy harvesting is one of alternative choices to solve this problem.

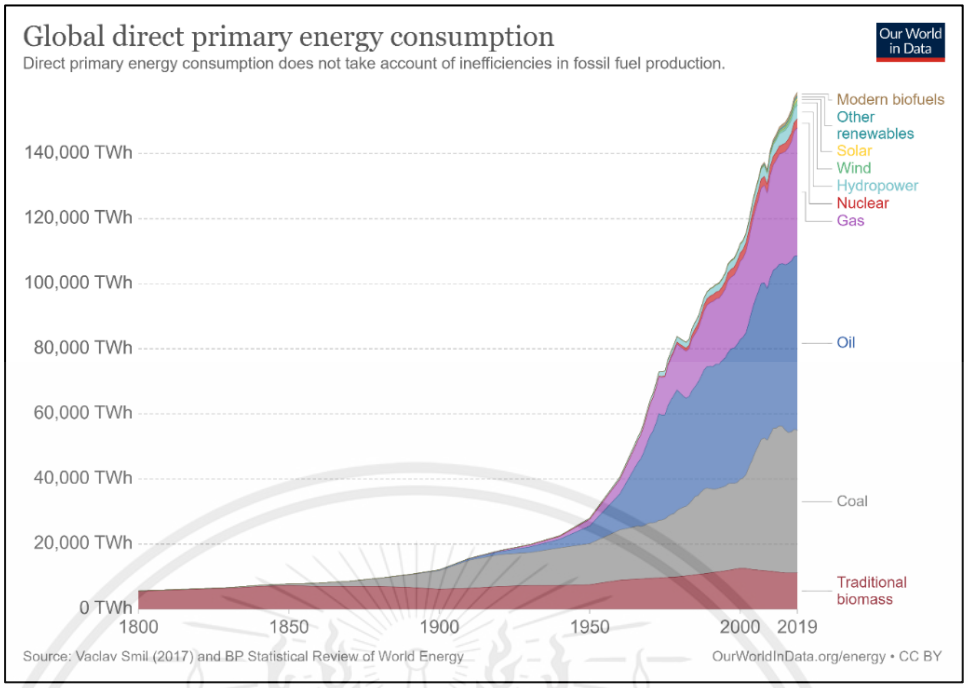

Figure 1-1: Global direct primary energy consumption 1800-2019[2]

Currently, many devices or systems such as battery, fermentation, and many electronic devices lose heat between processing. Thus, thermal energy is a suitable energy to harvest, especially low-grade heat source because the most of heat lose is in rage of low temperature(240 ^{o}C)[3]. In part of harvesting, energy harvesters have the main device which a role to transform difficult usable energy into easily usable energy (electric energy for current) such as solar cell, turbine, pyroelectric, piezoelectric, and etc. The energy harvester besides the main devices, there also needs a system to help for harvesting. Some systems use working fluid to drive the system as a harvester. Since, these fluids have the ability for harvesting and regeneration. For this reason, working fluid selection is a significant part of energy harvesting development and drives the world.

In summary, this project studies the working fluid of the energy harvesting system for low-grade heat sources by applying the data mining process to make an understanding of working fluid character in the database and filter the working fluids as candidates before the experiment.

1.2 Objectives

1. To construct mine of data for working fluid selection.
2. To take advantage of data mining in field of chemical engineer
3. To find interested candidate working fluids for future experiments.

1.3 Scopes of Work

1. Use substances contain in ProCAPE (computer Aided Tool for Property Estimation) database.
2. Interest azeotropic binary mixture and subcritical working fluid cycle.
3. Consider working fluids properties at 50^{o}C, normal boiling point lower or equal 100^{o}C.

1.4 Expected Outputs

1. Have mine of data for working fluid selection.
2. Get interesting working fluids for energy harvesting system experiment.

CHAPTER II

LITERATURE REVIEW

2.1 Working Fluid

Working fluid is fluid inside the boundaries of the system which can be liquid, vapor or gas[4]. The working fluid is separated to be pure working fluid and mixture working fluid.

Pure working fluid contains one compound. With being one compound, their lack of variety and has many limitations in term of operation condition, performance, safety, and environment. For working fluid selection should not consider only pure working fluid.[5]

Mixture working fluid contains two or more compound. The mixture working fluid has more alternative fluid than pure working fluid and wide range of operating conditions.[5] The mixture has two clearly character which is zeotropic mixture and azeotropic mixture. The zeotropic mixture is the mixture that does not contain the azeotropic point which shows the example Figure 2-1.[6] Zeotropic mixture working fluid accord advantages of the mixture working fluid at the above sentences. The azeotropic mixture working fluid is not variety equal to zeotropic working fluid but easier to control. Since, the azeotropic mixture can reduce effect of composition changing in term of operation, storage, or transportation.[7]

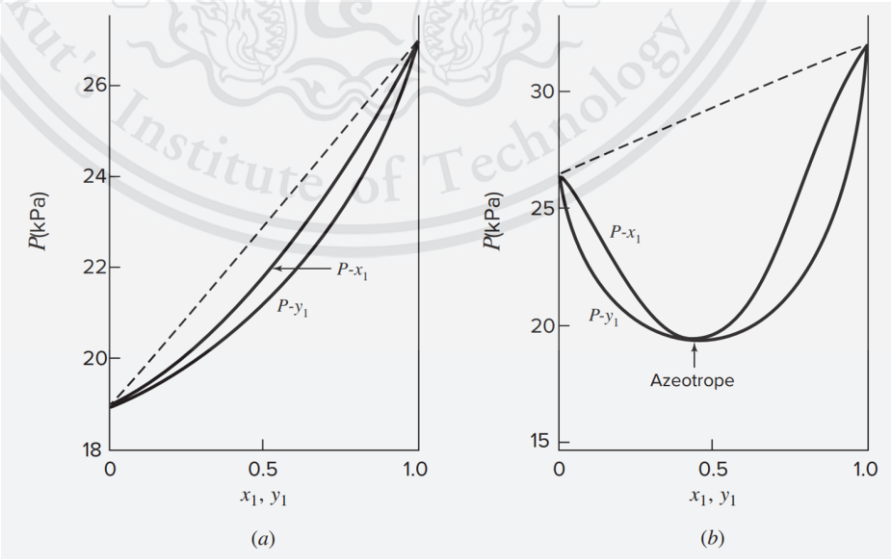

Figure 2-1: Pxy diagrams at constant T[6].

2.1.2 Practical use

The suitable working fluid of each cycle has different criteria however, it has the same common criteria. In Rankine-cycle, O. Badr et al.[8] concluded thermodynamic and physical criteria from suggestions by many author. Many suggestions can be the practical use for whole working fluid system which as follows.

1. Pressure for operating should not be high than mechanical stress of equipment and lower than atmospheric pressure which avoid equipment problem and air into the cycle.
2. Melting temperature of working fluid should be low to avoid solid phase in the system. This suggestion is considered when take advantage from vapor-liquid system.
3. Low heat capacity of liquid and high heat of vaporization reduce heat input to subcooled liquid before vaporization.
4. High liquid thermal conductivity and low liquid viscosity result in better performance of heat exchanger and reduce pressure drop in the pipe.
5. High specific volume both liquid and vapor consequent to heat transfer rate, huge size of equipment, and more pressure drop. In part of heat transfer, the properties have influent to heat transfer coefficient which depend on heat exchanger.
6. In part of safety, working fluid should be non-corrosive, stable, non-toxic, and non-flammability.
7. Lastly, working fluid is available and low cost.

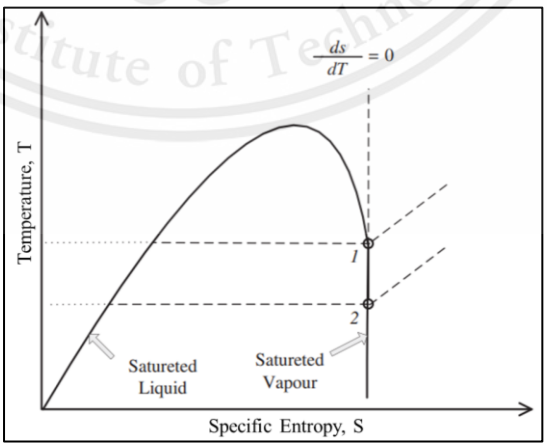

Figure 2-2: T-S diagram isentropic expansion and saturated vapor line[5]

W. su et al.[9] concluded various properties of working fluid that influent to organic Rankine Cycle which the most properties is according to O. Badr et al. The other properties were not mentioned. The other properties are as follows.

1. High boiling temperature result to better efficiency in organic Rankine Cycle.
2. High heat of vaporization is one part of declining required amount of working fluid. Another reason is ability of working fluid to store heat.
3. Low liquid heat capacity results in the saturated liquid line in T-S diagram which effect the cycle approach to Carnot-cycle.
4. Ozone depletion potential (ODP) and Global warming potential (GWP) are environment impact .ODP impact on ozone layer and GWP impact on greenhouse effect.
5. Molecular weight (MW) affects the efficiency of the turbine which high MW better the efficiency.

Both of O. Badr et al. and W. su et al. studied working fluid selection for Rankine cycle. Some points are reasonable for whole liquid-vapor cycle. However, working fluid depend on character of cycle.

2.2 Harvesting technique

Working fluid depends on the system which is the always emphasized sentence. For this section get to know the system for harvesting energy from low-grade heat source.

The Thermodynamic cycles are well-known techniques for energy harvesting. The various thermodynamic cycles are developed as power generation for low-grade heat sources such as Rankine cycle, Kalina cycle and trilateral flash cycle.[5] The principles is shown as follow.

1. Rankine cycle is similar Carnot cycle which solve operation of compression and expansion problems.[6] the cycle is show in Figure 2-3.
   1 to 2 is a constant pressure heating step in a reboiler.
   2 to 3 is an adiabatic vapor expansion step in a turbine.
   3 to 4 is a constant pressure condensing step in a condenser.
   4 to 1 is an adiabatic liquid compression step by a pump.

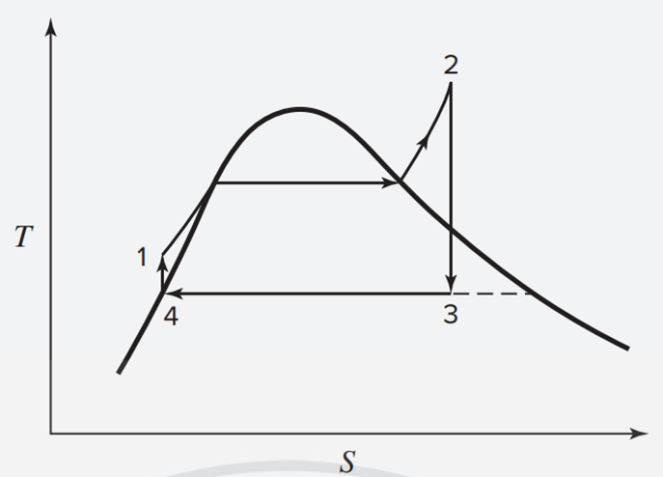

Figure 2-3: TS diagram of Rankine cycle.[6]

2. Kalina cycle is modified from Rankine cycle to manage irreversible mixture working fluid. Simplified Kalina cycle replace the condenser in Rankine cycle by other system which is called "Bottoming cycle".[10]
3. Trilateral flash cycle is Rankine cycle that without vapor generation while step of heating (1 to 2 in Figure 2-3).[11]

However, thermodynamic cycle efficiency depends on delta temperature of evaporator and condenser which affect very low efficiency or very low temperature of condensation for low-grad heat source. S. Monfray et al.12 attempted harvesting without additional electric energy .Their experiment generated power from thermal energy by piezoelectric via technique of thermomechanical conversion and thermofluidic conversion.[12]

Thermomechanical conversion applies the principle of bimetallic striping. Figure 2-4 show working principle of thermomechanical conversion which consist of two states operation. Up state, bimetal will rise the bimetal center until touch with the cold point. After that, the center descends at low state until touch the hot point and rise up again. This method make vibration to piezoelectric to generate electricity.[12]

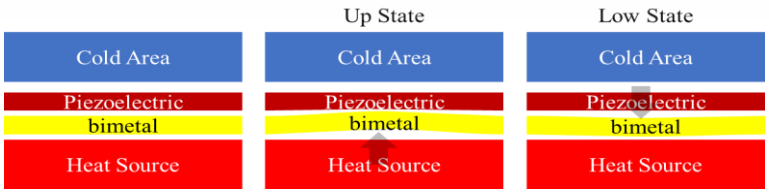

Figure 2-4: Thermomechanical conversion in S. Monfray et al.[12]

Thermofluidic conversion apply vapor-liquid phase change of working fluid. At start, the liquid is evaporated when touch hot surface after that the liquid drop is generated by vapor condensation and descends by capillary force and gravity forces. Evaporation occur again when the droplet touch hot surface. It makes oscillating of pressure inside container which result to vibration to piezoelectric.[12]

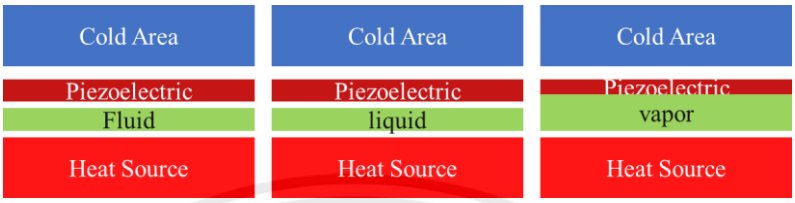

Figure 2-5: Thermofluidic conversion in S. Monfray et al.[12]

Both of thermomechanical and thermofluidic conversion has the key device as piezoelectric. This device contains piezoelectric material which generates an electric field when occurring strain. In contrast, electric field is applied to the material will deform the piezoelectric material. A simplified piezoelectric energy harvester consists of two parts which are generate electric energy (mechanical module) and converter and rectifier (circuit). Figure 2-6 illustrate phases of harvester.[13]

1. Mechanical-mechanical energy conversion
2. Mechanical-electrical energy conversion
3. Electrical-electrical energy conversion

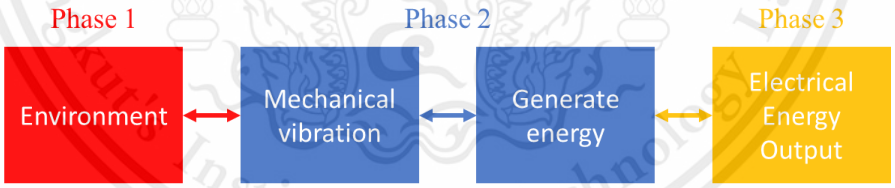

Figure 2-6: Phase of piezoelectric energy harvesting[13]

Hence, this project attend harvesting by piezoelectric device by the concept of thermofluidic conversion due to the system is low complex and use working fluid. In part of phase 1 of piezoelectric harvesting, two phase circulation loop thermosyphon (TPCT) is chosen for this project.

2.3 Thermosyphon

Thermosyphon in conventional application is used as a heat pipe without a pump in the system. The working fluid flow by gravity which fixes the position of the condenser at top of the evaporator.[14] The role of thermosyphon in this project is the

creation of working fluid circulation and applies mechanical strain to piezoelectric. Thermosyphon split in 3 type which illustrate in Figure 2-7.

a) Liquid circulation loop thermosyphon
b) Bubble lift thermosyphon
c) Two phase circulation loop thermosyphon (TPCT)

This project attend type c thermosyphon from Figure 2-7.

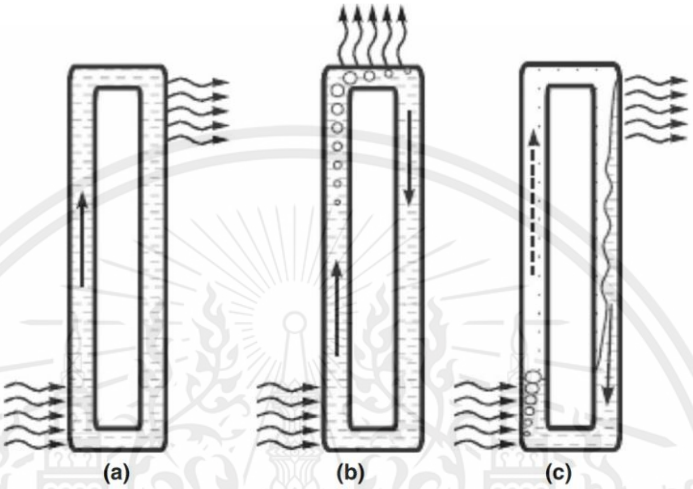

Figure 2-7: Type of thermosyphon[14]

2.3.2 Two phases closed loop thermosyphon operating principle

A TPCT starts by vaporizing working fluid at evaporator, then working fluid flows up throughout riser until condenser, then condense working fluid go down throughout downcomer then the evaporate again which show in Figure 2-8.[14]

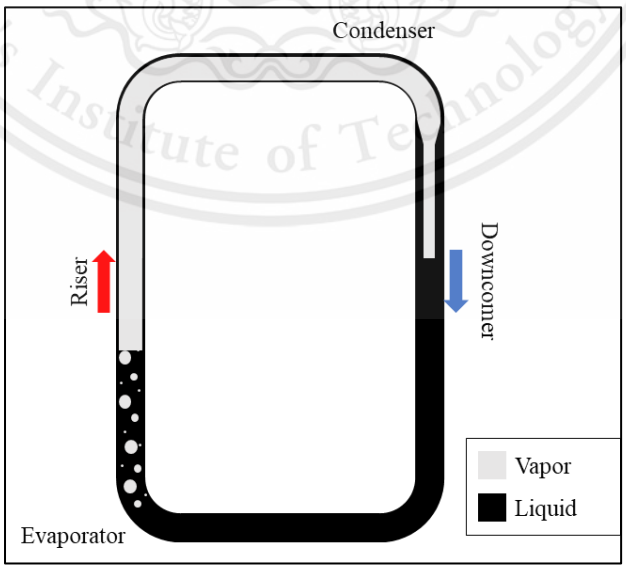

Figure 2-8: Two phase circulation loop thermosyphon[14]

For two phase system, the Bond number (Bo) is able to represent relation of two phases flow pattern and pipe diameter which define as.[15]

$$Bo=\frac{g(\rho_l-\rho_v)d_i^2}{\sigma}$$

For equation 2.1, Bo is the ratio of force act to the bubble between gravity and surface tension. A. Franco and S. Filippeschi[14] explained relation of flow pattern with diameter of pipe via Bo .The flowing of the working fluid in the TPCT riser when reducing diameter the bubble velocity will reduce until zero at Bo = 4. In physical meaning Bo < 4 is very high influence from surface tension force when compared with the gravitational force, another meaning Bo > 4, There is enough free space for generate bubble. In contrast, the diameter increasing result in the bubble velocity increasing until constant. Hence, the minimum and the maximum critical diameters are defined which are estimated by[14]

$$d_{cri,min}=2L_b$$

$$d_{cri,max}=19L_b$$

where,

$$L_b=\sqrt{\frac{\sigma}{g(\rho_l-\rho_v)}}$$

- $d < d_{cri,min}$ occurs flow regimes are symmetrical.[14]
- $d_{cri,min} < d < d_{cri,max}$ occurs flow boiling regime in the riser.[14]
- $d < d_{cri,max}$ occurs pool boiling in the riser.[14]

In case of diameter between maximum and minimum critical diameter, A. Franco and S. Filippeschi[16] found mass flow rate which is not according to increasing of heat flux due to rate of bubble generation is limited by space.

Relationship of sensible heat and laten heat is an interested parameter in phase change system. The Jakob number represent this relation which show in equation 2.5.[15] Jakob number affect to bubble growth rate which found by R. Cole, H. Shulman.[17]

$$Ja=\frac{C_p(T_s-T_{sat})}{h_{fg}}$$

2.3.3 Heat transfer

TCPT has key components as condenser and evaporator which are heat exchanger element. The working fluid affect the heat transfer rate by a parameter which called “heat transfer coefficient”.

In case of condenser, heat transfer coefficient according to the Nusselt theory for laminar flow is defined as[18]

$$h_{c,Nust}=0.943\left\{\frac{\rho_l g k_l^3(\rho_l-\rho_v)[h_{fg}+0.68C_{pl}(T_{sat}-T_s)]}{\mu_l(T_{sat}-T_s)L_c}\right\}^{1/4}$$

H. Hashimoto and F. Kaminaga found deviation of heat transfer coefficient from Nusselt theory calculation in TCPT condenser due to effect of liquid entrainment. Therefore, their heat transfer coefficient is defined as[18]

$$h_c=0.85Re_f^{0.1}\exp\left(-0.000067\frac{\rho_l}{\rho_v}-0.6\right)h_{c,Nust}$$

where,

$$Re_f=\frac{4Q}{\pi d h_{fg}\mu_l}$$

In case of evaporator, interesting regime of boiling is between natural convection regime with nucleate boiling. X is dimensionless pool parameter for as heat transfer regime criteria which proposed by S. EL-Genk and H. Saber. It is defined as.[18]

$$X=\Psi(RaPr_l)^{0.35}\left(\frac{P_v L_b^2 q}{\sigma\rho_v h_{fg}\nu_l}\right)^{0.7}$$

where,

$$\Psi=\left(\frac{\rho_v}{\rho_l}\right)^{0.4}\left[\frac{P_v\nu_l}{\sigma}\left(\frac{\rho_l^2}{\sigma g(\rho_l-\rho_v)}\right)^{1/4}\right]^{1/4}$$

Natural convection	$X < 10^6$	$h_{nat}=0.475\frac{k_l}{L_p}Ra^{0.35}\left(\frac{L_b}{d_i}\right)^{0.58}$
Two-phase convection	$10^6 \le X \le 2\times10^6$	$h_{TPC}=4\frac{k_l}{d_i}(ArFr^{0.5})^{1/3}Pr_l^{0.5}\left(\frac{Bo^{0.5}}{10}\right)^n$ $n = 1/2$ for $Bo^{0.5} \le 10$, $n = 1/6$ for $Bo^{0.5} > 10$
Two-phase convection	$2\times10^{6<}X \le 10^7$	$h_{TPC-NB}=\left(\frac{10}{8}-\frac{X}{8\times10^6}\right)^{\frac{3}{4}}h_{TPC}+\left(\frac{X}{8\times10^6}-\frac{2}{8}\right)^{\frac{3}{4}}h_{NB}$

Nucleate boiling	$X > 2.1\times10^{7}$	$h_{NB}=6.95\times10^{-4}(1+4.95\Psi)\frac{k_l}{L_b}\left(\frac{qPL_b^2}{\rho_v h_{fg}\nu_l\sigma}\right)^{0.7} Pr_l^{0.35}$

2.4 Property estimation model

Physical and thermodynamic properties are important data for working fluid. Property estimation model can split in 3 categories which are equation of state, group contribution method, and computational chemistry method. From Figure 2-9, the computational chemistry method is able to predict in the widest range of molecular structure but longtime calculation, which not lower than an hour for a molecule calculation. Since, the calculation is deep in the atomic scale. In case of equation of state, The most of equation of sate models have been developed for thermodynamic properties and few molecules can predict by equation of sate due to various values in equation of state have been confirmed by experiment.[9]

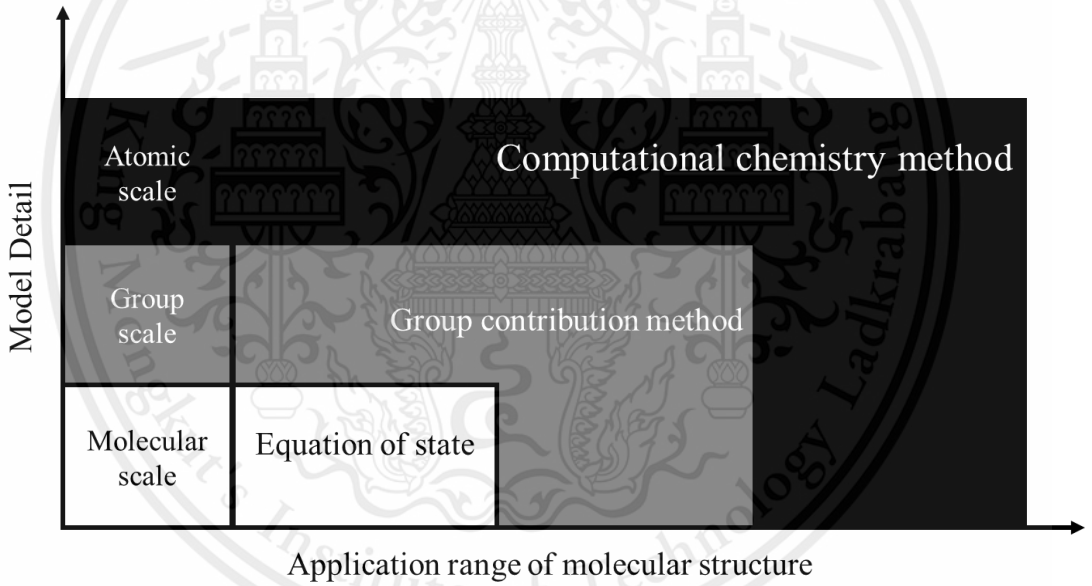

Figure 2-9: Ability of property prediction model[9]

2.4.2 Prue property estimation

This project uses a simplified mixing rule for the mixture properties, thus pure properties are necessary for the mixing rule. The group contribution methods play an important role in pure properties estimations.

This project uses pure property estimation in ProCAPE (product of PSE for speed), which contains group contribution methods of Marrero & Gani, Constantinou & Gani, Joback & Reid, and Wilson. To fulfill the lack of data in the database. The data

lack includes liquid heat capacity, liquid dynamic viscosity, and liquid thermal conductivity.

Liquid heat capacity bases on Rowlinson-Bondi equation is defined as:[9]

$$C_p^l = C_p^{ig} + R\left(1.45 + \frac{0.45}{1-Tr}\right) + 0.25\omega\left(17.11 + 25.2\frac{(1-Tr^{1/3})}{Tr} + \frac{1.742}{1-Tr}\right)$$

where, ideal gas heat capacity from Joback and Reid method which is temperature polynomial[9]

$$C_p^{ig} = A + BT + CT^2 + DT^3$$

Liquid dynamic viscosity based on Constantinou & Gani, or Joback & Reid methods which base on Andrade equation.[9]

$$\mu_i = \exp\left(\frac{A}{T} + B\right)$$

Liquid thermal conductivity can predict by all methods in ProCAPE. Prediction of thermal conductivity is not successful theory. Therefore, the thermal conductivity prediction has been developed by approximation from engineer calculation. Two type of approximations are calculation parameters in function by group contribution method and another is prediction relation between thermal conductivity and temperature from a reference point.[9]

2.4.3 Thermodynamic model

Modified Raoult's law is equation 2.17 which use to predict behavior of vapor liquid equilibrium. The equation requires an important parameter which is called "activity coefficient". Many models are able to calculate but need interaction parameters between compounds in the mixture. UNIFAC is different which calculate the parameter by group contribution concept. This project uses original UNIFAC and KT-UNIFAC first order. The original UNIFAC method is as follows(equation 2.18-2.29).[6]

$$Py_i = P_i^{sat}\gamma_i x_i$$

$$ln\gamma_i = ln\gamma_i^C + ln\gamma_i^R$$

UNIFAC is sum of combinatorial term (c: effect of molecular size and shape differences) and residual term (r: effect of interaction) which depends on subgroups. The subgroups are structural units form molecules of a solution.[6]

$$\ln\gamma_i^C = 1 - J_i + \ln J_i - 5q_i\left(1 - \frac{J_i}{L_i} + \ln\frac{J_i}{L_i}\right)$$

$$\ln\gamma_i^R = q_i\left[1 - \sum_k\left(\theta_k\frac{\beta_{ik}}{s_k} + e_{ki}\ln\frac{\beta_{ik}}{s_k}\right)\right]$$

where,

$$J_i = \frac{r_i}{\sum_j r_i x_i}$$

$$L_i = \frac{q_i}{\sum_j q_i x_i}$$

$$r_i = \sum_k v_k^{(i)} R_k$$

$$q_i = \sum_k v_k^{(i)} Q_k$$

$$e_{ki} = \frac{v_k^{(i)} Q_k}{q_i}$$

$$\beta_{ik} = \sum_m e_{mi}\tau_{mk}$$

$$\theta_k = \frac{\sum_i x_i q_i e_{ki}}{\sum_j x_j q_j}$$

$$s_{ik} = \sum_m \theta_m \tau_{mk}$$

$$\tau_{mk} = \exp\frac{-a_{mk}}{T}$$

KT-UNIFAC first-order model replace equation 2.30 by equation 2.31 which include the effect of temperature on interaction parameter.[19]

$$\tau_{mk} = \exp\frac{-\left[a_{mk,1} + a_{mk,2}(T - T_0)\right]}{T}$$

where,

R, Q subgroup parameter

i identifies compound

j dummy index running over all compounds

k identifies subgroup

m dummy index running over all subgroups

2.5 K-means clustering

Clustering is partitioning of large data to many smaller data. K-means is the most popular algorithm. K-means get the input as number cluster and then random centroids in amount of data. Number of the centroids is equal the input value. The centroid positions are calculated and optimized until stable or achieve number of rounds.[20]

Elbow method is used to input suitable number of clusters by graphical method. The graph is plotted between sum of distance (between data with its centroid is also call sum of squares) with number of clusters. The distance will be decrease as a number of clusters increase and the slope will decrease. Therefore, the graph character is an elbow. The number of clusters at the highest delta slop is a suitable point for elbow method. Since, if lower than this point result to more variance in data of each cluster and if higher than this point increase risk of over fitting problem.[21]

CHAPTER III

RESEARCH METHODOLOGY

3.1 Overall process

Data of this project is managed by coding via python in visual studio code. The overall process is visualized via flow chart in Figure 3-1.

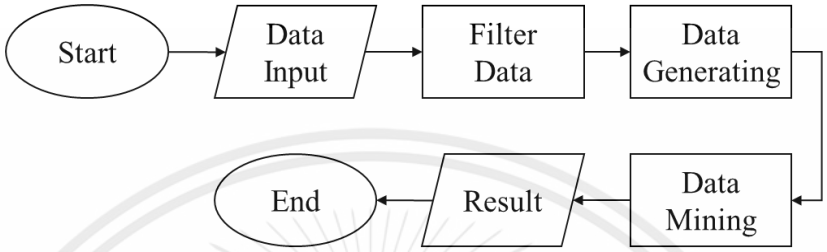

Figure 3-1: Overall flowchart

The flow starts at the data input from ProCAPE database includes index (identify compound), constant properties (such as critical point, omega, normal boiling point, and etc.), correlation properties (the function of temperature). Next, data filter by common criteria for working fluid selection and then, data-generating uses thermodynamic model and pure properties estimation. Lastly, data mining applies clustering by K-means method and show the result by visualization. In filter data, the eliminated data is melting temperature more than 18^{o}C (avoid solid phase in system), critical temperature more than (scope of work study subcritical), normal boiling point more than water (due to very high normal boiling point result in mixture working fluid more chance lower operating pressure than atmospheric), and duplicated UNIFAC subgroup data.

3.2 Data-generating

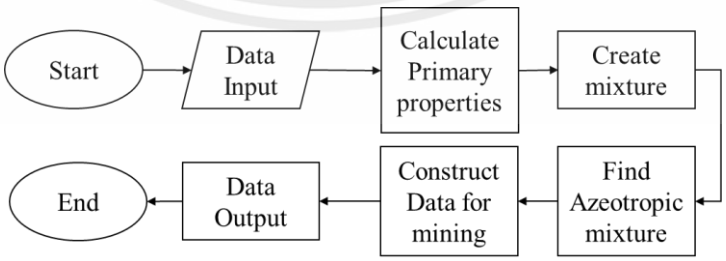

Figure 3-2: Data-generate flowchart.

From Figure 3-2, Data input from filtered data and calculate involve correlation properties at 50°C as primary properties which show in Table A-1 and Table A-2. Next, combined pure compound data for the mixture creation and find azeotropic mixture. Construct data for mining is primary properties calculation by simplified mixing rule and add safety data from outer source in appendix Table A-3.

3.2.2 Find azeotropic mixture.

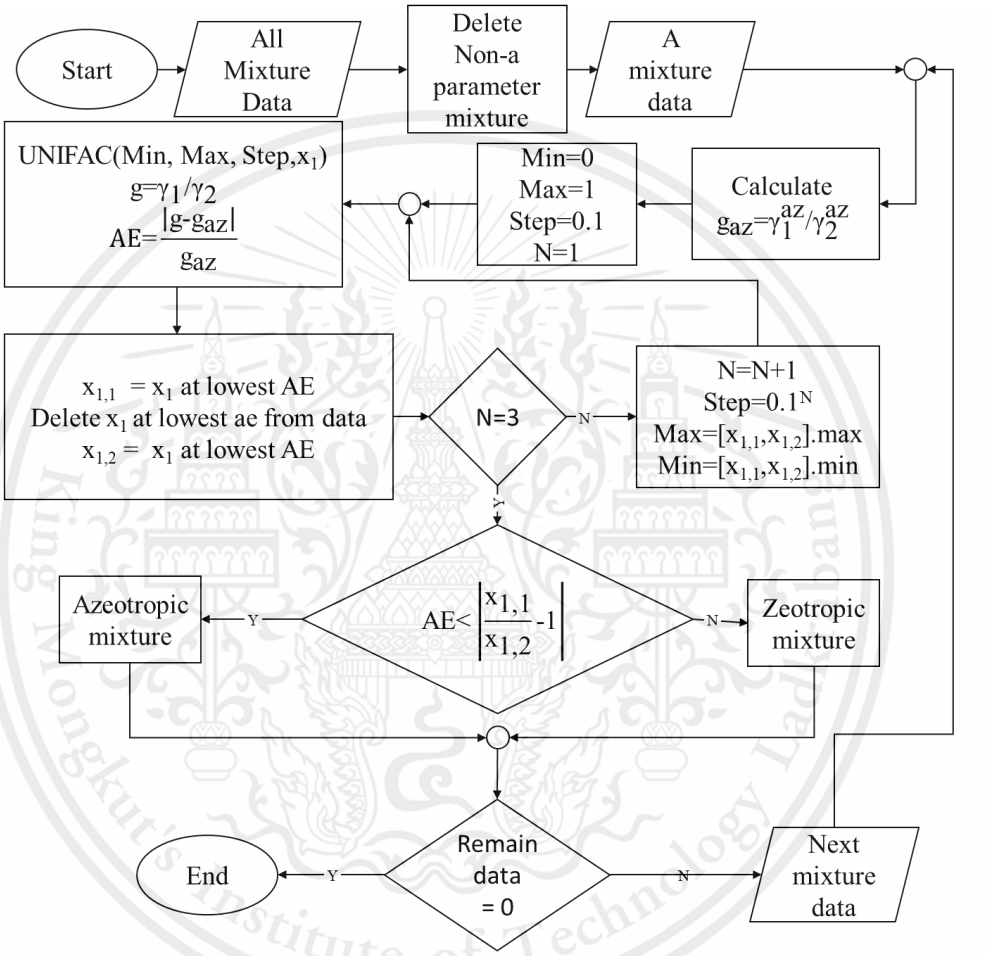

Figure 3-3: Find azeotropic mixture flowchart.

Figure 3-3 show flowchart of azeotropic mixture finding. Where, Min is minimum value, Max is maximum value, Step is stepping value, and N is run number. For g_{az} calculation, modified Raoult's law is applied in this part. For azeotropic deciding, mixture is decided by comparing absolute error of g with the most possible absolute error. The most possible absolute error is calculated by absolute error between $x_{1,1}$ and $x_{1,2}$. Since y_1 is equal to x_1 at azeotropic point, thus the most deviation value of y_1 is $x_{1,2}$ when x_1 is equal to $x_{1,1}$.

3.2.3 Involved properties.

The importance properties are separated in two parts which are primary properties and secondary property.

Primary properties are working fluid properties from calculation of correlation properties which affect to system. The properties include vapor density, liquid density, liquid heat capacity, heat of vaporization, liquid dynamic viscosity, surface tension, and liquid thermal conductivity.

Secondary properties are values that calculate from primary properties and affect to system which include bond number, jakob number, dimension less pool parameter, heat transfer coefficient at evaporator, and heat transfer coefficient at condenser.

3.3 Data mining

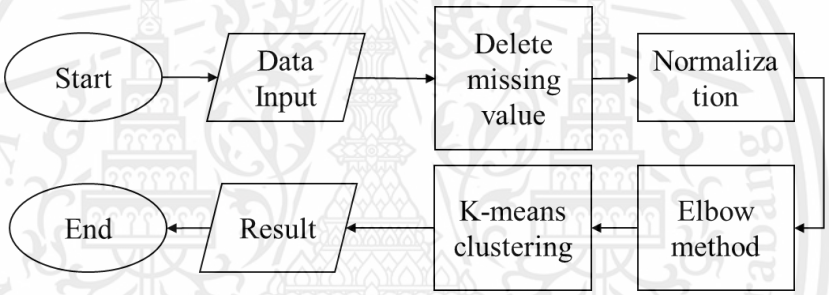

Figure 3-4: Data mining flow chart

Data mining start by input azeotropic mixture data after that delete the mixture data that contain missing value. Data is normalized by equation 3.1 for eliminate bias of each data and use elbow method to find number of clusters for K-means clustering. Lastly, result visualization by radar char (equation 3.2) with 5% percentile, mean value, and 95%percentile.

$$D_{norm} = \frac{D - D_{mean}}{D_{std}} \quad 3.1$$

$$D_{plot} = \frac{D - D_{min}}{D_{max} - D_{min}} \quad 3.2$$

CHAPTER IV

RESULTS AND DISCUSSION

4.1 Results of data mining

Results of data mining by K-mean clustering are shown in Figures 4-1, 4-2, and 4-3 which are primary properties, secondary properties, and safety respectively. Each radar chart (a) is plotted by the values of 5 percentiles, means, and 95 percentiles. Each bar chart show number of members in each cluster. K-mean clustering is clustering by distance calculation between each data point with centroid points which the results as centroid points and other data for clustering are reported in appendix B.

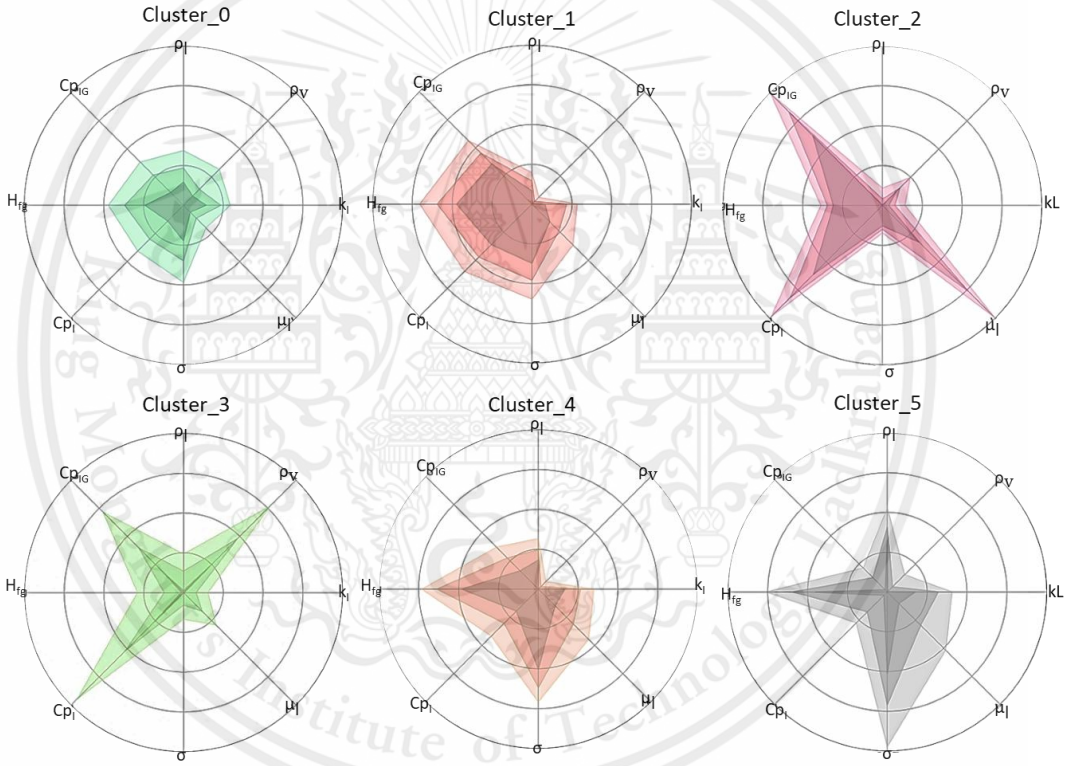

(a)

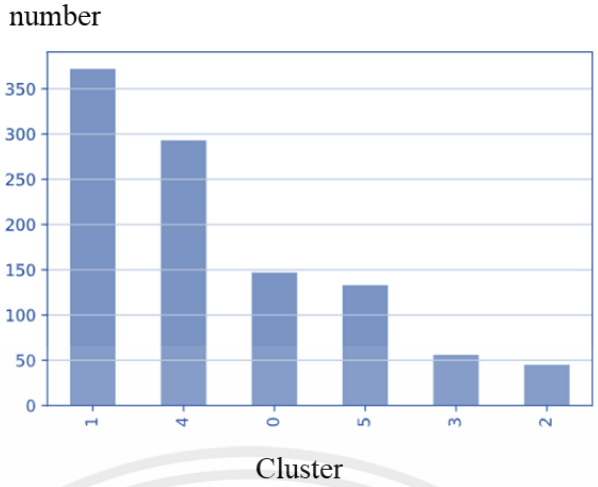

(b)

Figure 4-1: (a) The character of each primary properties cluster on each radar chart/ (b) The member number of each primary properties cluster on a bar chart

From Figure 4-1, The mixtures are clustered in 6 clusters with based primary properties. For cluster 0, all primary properties are lower than 50% when compared with other clusters, particularly liquid viscosity. Both the cluster 1 and cluster 4 have the most members and quite similar characters. The characters deviate on the bottom left of the radar charts as the same which differ at the points of the heat capacities of the liquid and ideal gas that cluster 4 is less than. Cluster 2, 4, and 5 have quite unique characters. For cluster 2, It is the smallest membership cluster, which character includes high-value properties (liquid, and ideal gas heat capacities), low-value properties ([25%-50%: latent heat]; [<25%: densities, thermal conductivity, and surface tension]), and wide range properties (25%-100%: liquid viscosity). Each member of cluster 2 is quite similar which reflects from the gap between the line of 5 and 95 percentile on the radar chart when compared with other clusters. Shape of cluster 3 in Figure 4-1 (a) resemble cluster 2 which differ points are liquid viscosity and density of vapor. Character of cluster 5 consists of high-value properties (surface tension, and latent heat), low-value properties ([25%-50%: liquid density]; [<30%: vapor density, liquid, and ideal gas heat capacity, and surface tension]), and wide range properties (10%-50%: liquid viscosity, thermal conductivity).

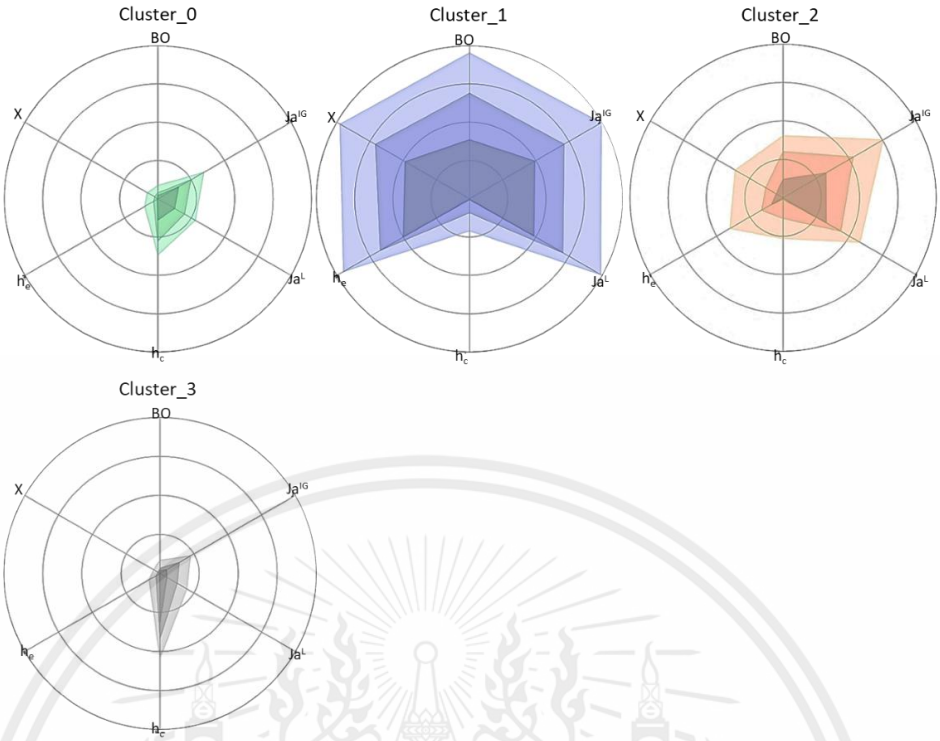

(a)

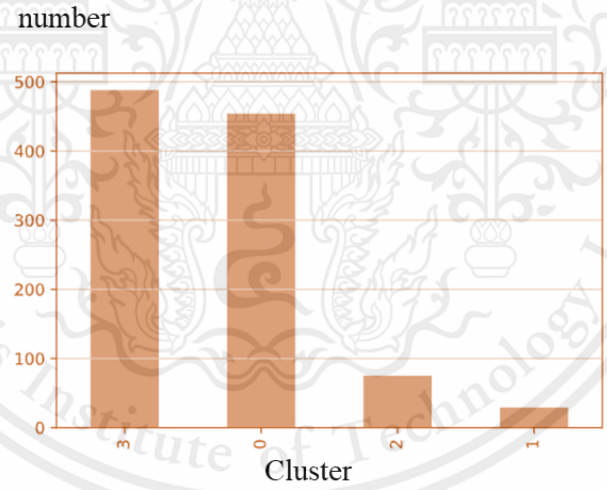

(b)

Figure 4-2: (a) The character of each secondary properties cluster on each radar chart/ (b) The member number of each secondary properties cluster on a bar chart

Secondary properties clustering includes 4 clusters which are shown as radar plot and bar chart in Figure 4-2(a), and Figure 4-2(b) respectively. Most mixtures are clustered in clusters 3 and 0. Cluster 2 and 1 have members about 10% of the total mixture. Cluster 0 is less on every side specifically properties that associate with the performance of heat transfer in the evaporator. Cluster 1 is in contrast with cluster 0

which has the highest maximum values and wide range on every side but except h_c. For cluster 2, the shape of each level in the radar plot is rather different which trend toward high Jakob numbers. The radar plot shape of cluster 3 is similar to cluster 0 but Jakob numbers are lower than and h_c is higher than.

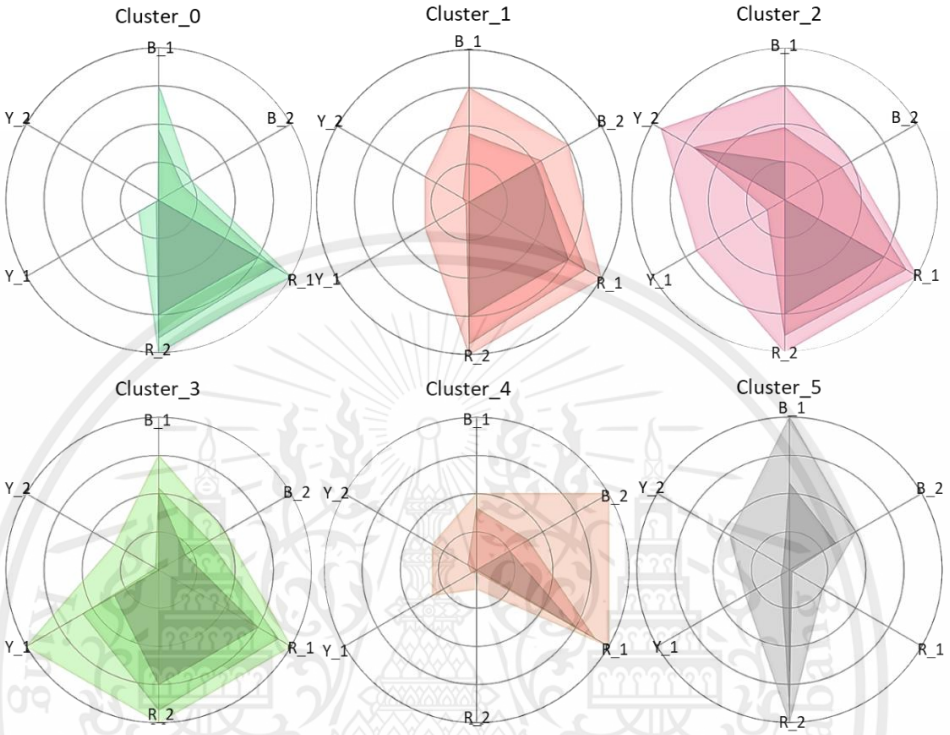

(a)

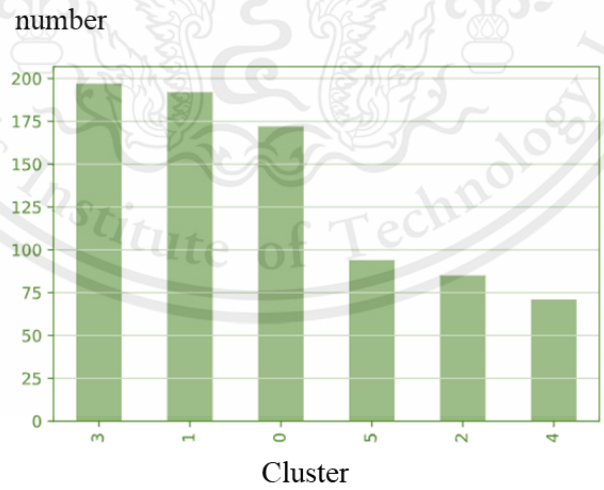

(b)

Figure 4-3: (a) The character of each safety cluster on each radar chart/ (b) The member number of each safety cluster on a bar chart

When, B: blue in NFPA 704, R: red in NFPA 704, Y: yellow in NFPA 704,

1: compound 1, compound 2.

Safety clustering considers NFPA 704 which is split into 6 clusters in Figure 4-3. In the bar chart, the cluster is clearly separated into two groups which one has more than 100 mixtures (0, 1, and 3) and another has less than 100 mixtures (5, 2, and 4). From clustering, clusters 0, 1, 2, and 3 consist of mixtures of flammable compounds which differ from clusters 4, and 5 that contain mixtures of a flammable compound with a non-flammable compound together. Cluster 0 apar from flammable mixture contains compound 1that health hazard in the mixture. Cluster 1 is similar to cluster 0 but has the health hazard in compound 2. Cluster 2 is rather harmful mixtures which contain health hazard, flammable, and unstable mixture. Cluster 3 is similar to cluster 2 but compound 2 is softer in terms of health hazard and stable compounds. For cluster, and 5. Both of them are similar in that cluster 4 contains flammable compound 1 and health hazard compound 2, cluster 5 has flammable compound 2, and health hazard compound 1.

4.2 Model applying

Model applying is applying the model to past experiments by various scholars. Where all compounds in those experiments are presented with their cluster in Table 4-1.

Table 4-1: Primaries properties and secondaries properties cluster of other compounds.

Compound	Primaries properties	Secondaries properties
water	5	0
ethanol	5	0
triethylene glycol (teg)	2	3
R113	1	1
R12	3	1
R134A	3	1
R141b	4	1
R11	4	1

T. Kiatsiriroat, et al. studied the performance of thermosyphon with binary working fluids in the application as heat pipe. The study associated with water, ethanol, TEG, and mixtures of water. Results of the experiment are shown on Figure 4-4, and

Figure 4-5.[22] Whether they be Figure 4-4 or Figure 4-5, results of pure water rather close to pure ethanol which compare with the result of pure TEG rather differ. From Table-4-1, ethanol and water are clustered in the same cluster both of primaries and secondaries properties but TEG is different which according to the result of T. Kiatsiriroat, et al. From Figure 4-4, The temperature profile of TEG is a rather wide range when compared with others. It can be explained with primary and secondary properties. Cluster 5 (water and ethanol) is high latent heat than cluster 2 (TEG) which resulted in the profile is stable due to the most of energy is spent to change the phase more than change temperature which confirms again with Jakob number in secondary properties of cluster 0 and 1. Thermal resistance and heat transfer rate in a Figure 4-5 can be interpreted with heat transfer of evaporator and dimensionless pool parameter. h_e and X a bit differ in clusters 0 and 3 in secondary properties. Cluster 3 is lower values than cluster 0, thus TEG is bad heat transfer in evaporator.

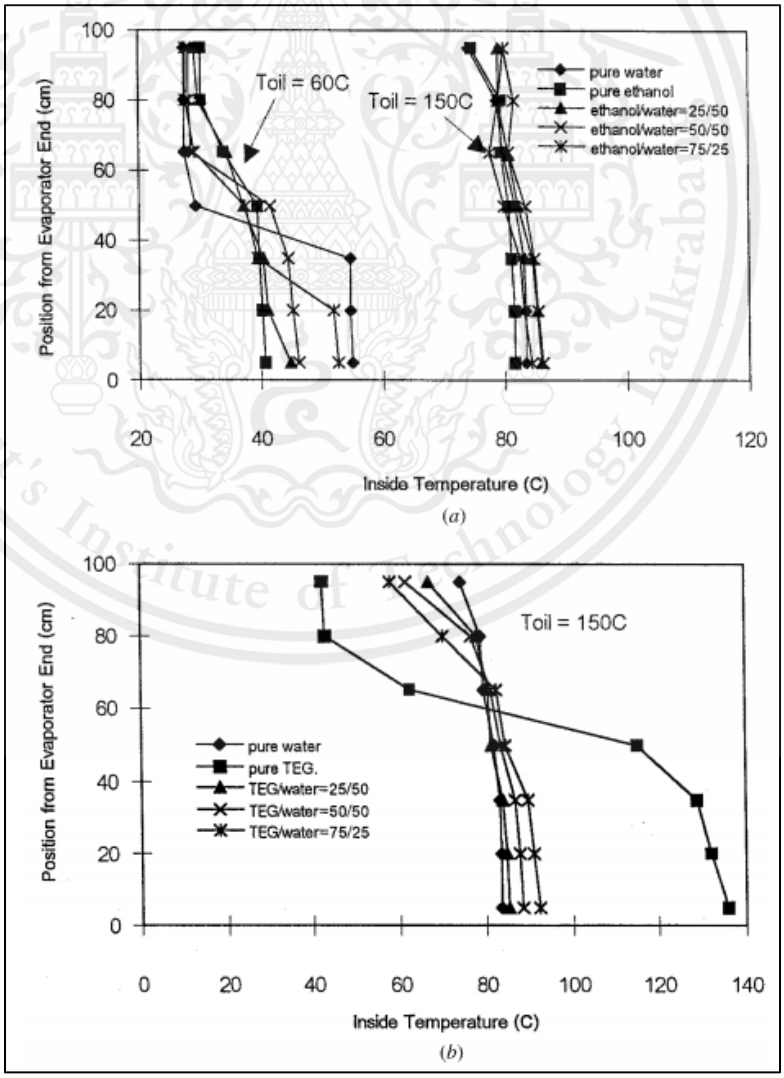

Figure 4-4: Temperature profile in evaporator at various condition

Where, (a) ethanol-water; (b) TEG-water.[22]

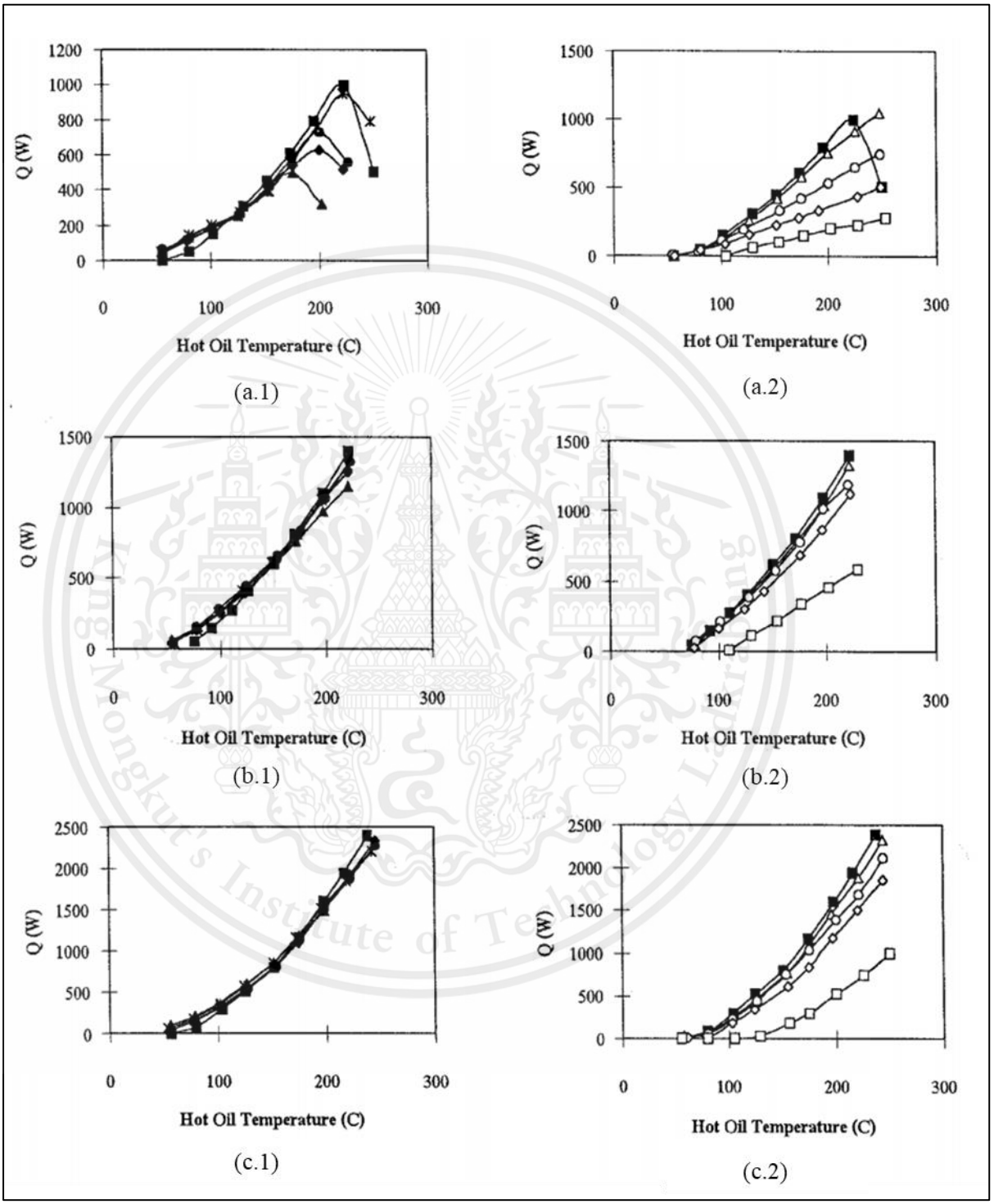

(I)

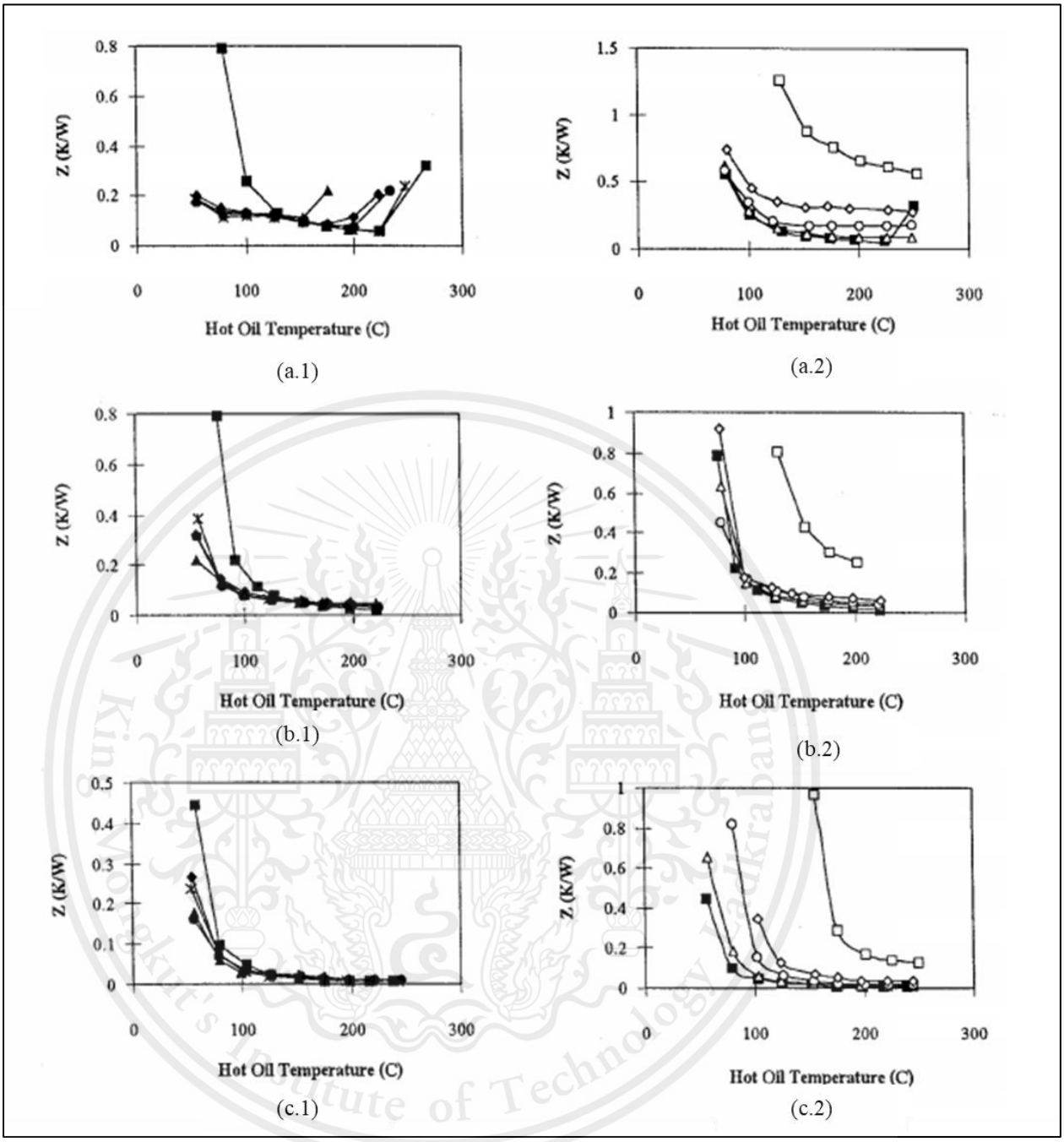

Figure 4-5: Relation of hot oil temperature with heat transfer rate (Q) and thermal resistance (Z) of thermosyphon in experiment of T.Kiatsirroat et al.[22]

Where, I : plot hot oil temperature with heat transfer rate

II : plot hot oil temperature with thermal resistance

III: legend in both graphs.

1 : ethanol-water

2 : TEG-water

a : tube diameter 12.70 mm

b : tube diameter 19.05 mm

Due to the fluid flow into condenser often have vapor fraction less than one which means liquid entrains the condenser. Hence, H. Hashimoto and F. Kaminaga studied the effect of entrainment on heat transfer.[23] For the condenser, the heat transfer coefficient in the condenser is a direct parameter. For secondary properties, water and ethanol are clustered in cluster 0 and R-113 is cluster 1. The h_c of both is similar which result in Figure 4-6 show condensation number is close between 0.1 to 0.3.

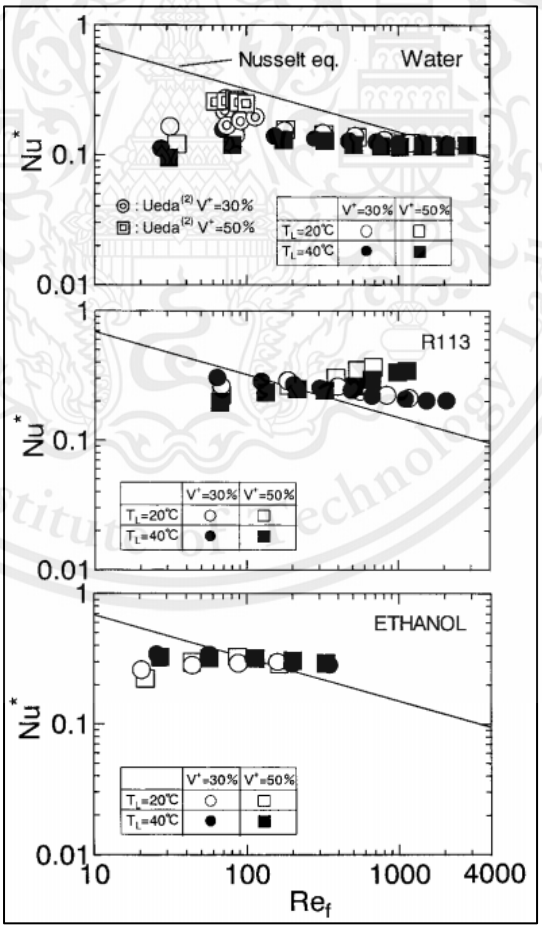

Figure 4-6: Condensation number and film Reynolds number at the condenser.[23]

J. Enaburekhan and U. Yakasai set experiment to study the performance of solar water heater of R-12, R-134A, and ethanol in Northern Nigeria.[24] The Figure 4-7 and 4-8 show the results in different sky conditions. R-12 and R-134a are cluster 3 and cluster 1 for primary and secondary properties respectively. The results conflict with clustering which results of R-134A and R-12 should close together. However, secondary properties cluster sufficiently to explain. As previously compared, h_c of clusters 0 and 1 are close but the minimum value is cluster 1. R-12 possible to be the side of the minimum value which influent to the temperature of the water was low. R-134a gave the highest water temperature especially the clear sky situation which effects from good heat transfer in the evaporator (h_e and X)than cluster 0. When heat transfer in the evaporator is the performance that means can carry energy more than cluster 0 which affect to water temperature in condenser.

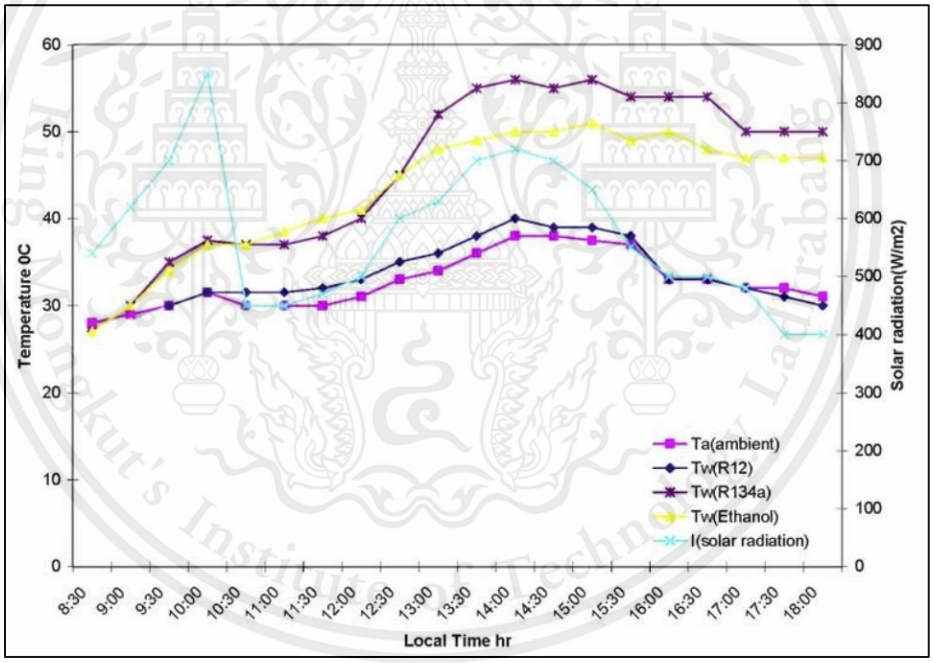

Figure 4-7: Comparing solar radiation with water temperature (condenser) of various working fluids in partial clouded day.[24]

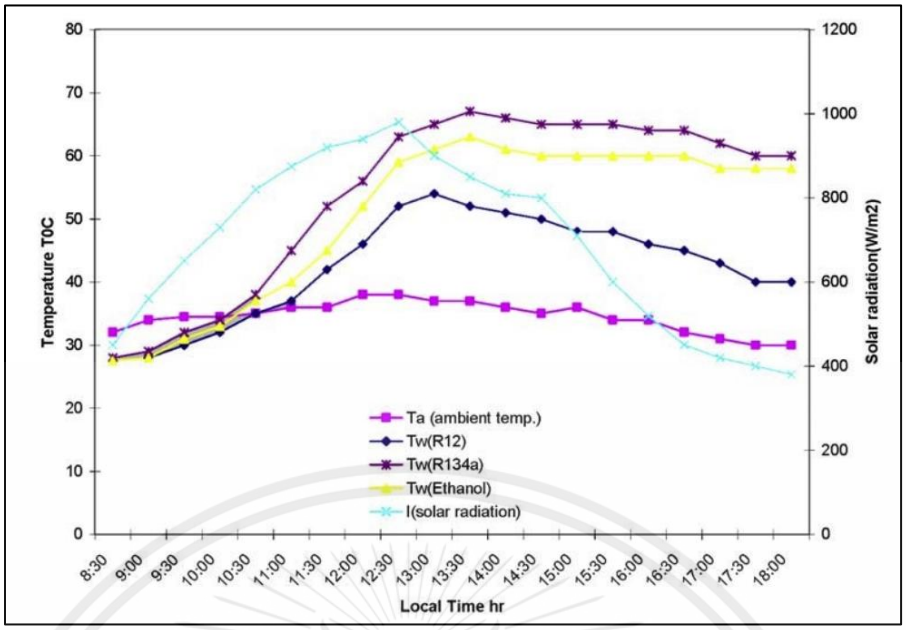

Figure 4-8: Comparing solar radiation with water temperature (condenser) of various working fluids in partial clear sky day

A. Franco study heat transfer and flowing of two phase thermosyphon.[25] Some result is shown in Figure 4-9 which is relation of mass flow rate and heat input. From Figure 4-9, water clearly deviated from others, mass flow rate of R-141b and R-11 did not increase after heat input more than 150 w, but R-113 still increased. This result is rather agreeable with clustering. Water is clustered differently from others which is clusters 5 and 0 for primary and secondary properties. Cluster 5 has the high value of latent heat and cluster 0 gives poor heat transfer for the evaporator, thus require high energy to drive water. R-141b, R-11, and R-113 are clustered in cluster 1 for secondary properties but for primary properties, R-113 is cluster 1 and the others are cluster 4. Mass flow rate can be affected by Bond number (equation 2.1) but R-141b, R-11, and R-113 are the same secondary properties cluster but different in primary properties. For primary properties, delta densities of liquid and vapor of clusters 1 and 4 are close but surface tensions are opposite which cluster 4 is higher. High surface tension affects low Bo which influents to the relation of mass flow and heat input.

$$Bo=\frac{g(\rho_l-\rho_v)d_i^2}{\sigma} \qquad 2.1$$

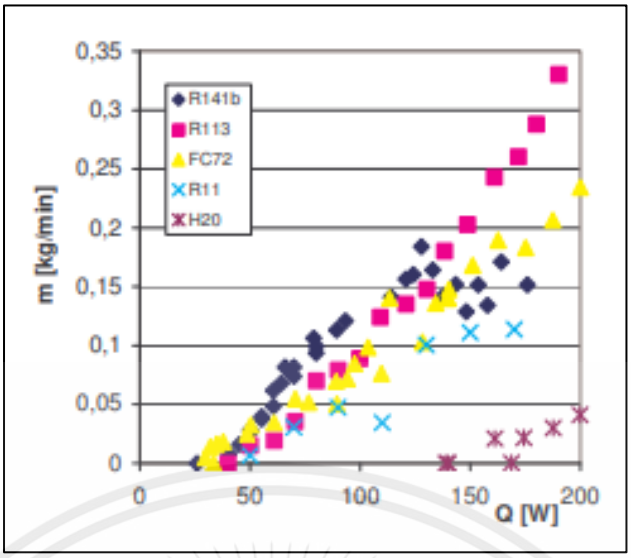

Figure 4-9: Mass flow rate and heat input of various working fluids.[25]

4.3 Interested working fluids.

For the design experiment for selecting working fluid, the working fluid should come from different clusters to study various effect from each cluster. However, safety is importance thus mixture cluster 4 and 5 is interested. Furthermore, the mixtures in cluster 4 should high composition of compound 2 due to safer than compound 1 but the cluster 5 is contrast. Therefore, considered secondaries and primaries properties are showed in table 4-2.

Table 4-2: Primaries and secondaries properties in cluster 4 and 5 of the safety clustering for the database.

Secondaries / Primaries	0	1	2	3
0	✓			
1	✓		✓	
2			✓	
3		✓	✓	
4	✓			✓
5				✓

From table 4-2, at least 9 mixtures are chosen from 1,074 azeotropic mixtures for the experiment design which hope to disparate result in each cluster. The candidate is shown on table 4-3.

Table 4-3: Candidate mixtures for each cluster.

No	Primary cluster	Secondary cluster	Safety cluster	Compound 1	Compound 2	P_{az} (bar)	x_1
1	0	0	5	R-114	n-Butane	5.19	0.57
2	1	0	4	Acetone	R-123a	2.08	0.01
3	4	0	4	Ethanol	R-11	2.35	0.02
4	3	1	4	R-12	R-218	17.00	0.25
5	1	2	5	R-C318	Cis2-Butene	8.26	0.58
6	2	2	4	Cyclobutane	R-3-1-10	6.06	0.35
7	3	2	4	R-152a	R-134a	13.48	0.33
8	4	3	5	R-21	Cyclobutane	3.98	0.90
9	5	3	5	R-30	Cyclopentane	1.49	0.80

Since the harvesting technique of this project intent to apply the application of piezoelectric as mention in chapter 2. When considering the energy converting, piezoelectric generates electricity from deformation by applying mechanical energy. The important things are amplitude and frequency which are vapor expansion and rate of flow respectively in the aspect of the working fluid. For liquid-vapor expansion, No. 4 and 7 in table 4-3 are interesting due to is in cluster 3 of primary properties but too much expansion can break the piezoelectric. For flow rate, the important things should be considered in two part as the part of ability of flow and limit of flow. For the ability, many parameters are associated whether they be latent heat, viscosity, heat transfer coefficient, and etc. For the limit of flow, Bo is an important parameter. No. 4 still gives interesting properties due to low latent heat, low viscosity, and high ability of heat transfer in the evaporator but a problem is probably about the limit of flow. Hence, No. 7 is an alternative for the higher energy source. However, No. 4 and 7 are poor heat transfer in the condenser, which result to the unstable system, which require more supplier than the others for high energy source or the large aera of the condenser. No. 8 and 9 probably give results disparate with 4 and 7 with high latent heat and good heat

transfer in the condenser. However, this discussion is extrapolation results from properties which be result of clustering which help to desire experiment.

CHAPTER V

CONCLUSION

5.1 Conclusion

In summary, this project use data of working fluid that associate with harvesting energy by thermosyphon which passes the process of generating data by group contribution method and mining data by machine learning as K-mean cluster to help design experiment. The clustering is split into 3 groups which are primary properties, secondary properties, and safety. Primary and secondary are applied in past experiments of other scholars to study the relationship of clustering with the results. From the study, the results are consistent with the clustering which means working fluid in the same cluster will give similar results. Although, some results need to interpret but still have the reason. Therefore, experiment design can use clustering with interpretation to study the impact of working fluid on the system which help to reduce waste and cost from experiments. In term of the harvesting system, the 9 mixtures are chosen from 1,057 azeotropic mixture as the candidates which consist of R-114 with n-Butane, Acetone with R-123a, Ethanol with R-11, R-12 with R-218, R-C318 with Cis2-Butene, Cyclobutane with R-3-1-10, R-21 with Cyclobutane, and R-30 with Cyclopentane.

5.2 Suggestion

1. This clustering is used for thermosyphon. Other system should consider the parameters especially parameter in secondary properties.
2. Scope of conditions and working fluids should be in the range of scope but still, can work out of scope.
3. For clustering, the weight of each parameter affects clustering which this project uses the same weight for all parameters by normalization.
4. Properties calculation uses the simple mixing rule which is not suitable for the mixture of polar substances. Thus, the property values deviate from the calculation.
5. The candidates were considered safe as a priority which are possibly not the good represent mixtures in terms of properties.

REFERENCES

(1) Ii, B. A. B. Data Mining Data Mining. *Min. Massive Datasets* **2005**, *2* (January 2013), 5–20. https://doi.org/10.1002/9781118445112.stat06466.pub2.

(2) Global Change Data Lab. Global direct primary energy consumption https://ourworldindata.org/grapher/global-primary-energy?time=earliest..2019 (accessed Nov 19, 2020).

(3) Kishore, R. A.; Priya, S. A Review on Low-Grade Thermal Energy Harvesting: Materials, Methods and Devices. *Materials (Basel).* **2018**, *11* (8). https://doi.org/10.3390/ma11081433.

(4) Eastop, T. D.; McConkey, A. Introduction and the Frist Law of Thermodynamics. In *Applied Thermodynamics: For Engineering Technologists*; PearsonEducation Limited, 1993; Vol. 18, pp 1–9. https://doi.org/10.1080/03043799308923249.

(5) Bao, J.; Zhao, L. A Review of Working Fluid and Expander Selections for Organic Rankine Cycle. *Renew. Sustain. Energy Rev.* **2013**, *24*, 325–342. https://doi.org/10.1016/j.rser.2013.03.040.

(6) Smith, J. M.; Van Ness, H. C.; Abbott, M. M.; Swihart, M. T. *Introduction to Chemical Engineering Thermodynamics*, 8th ed.; Weber, J., Avenarius, L., Neyens, L., Bies, L., Hillebrand, R., Schnee, S., Fuller, L. M., Shaqir, E., Homer, M., Seegmiller, M., Eds.; McGraw-Hill Education, 1950; Vol. 27. https://doi.org/10.1021/ed027p584.3.

(7) FUKUSHIMA, M. AZEOTROPIC OR AZEOTROPE - LIKE COMPOSITION , WORKING FLUID FOR HEAT CYCLE , AND HEAT CYCLE SYSTEM. US 2020/0148930 A1, 2020.

(8) Badr, O.; Probert, S. D.; O'Callaghan, P. W. Selecting a Working Fluid for a Rankine-Cycle Engine. *Appl. Energy* **1985**, *21* (1), 1–42. https://doi.org/10.1016/0306-2619(85)90072-8.

(9) Su, W.; Zhao, L.; Deng, S. Group Contribution Methods in Thermodynamic Cycles: Physical Properties Estimation of Pure Working Fluids. *Renew. Sustain. Energy Rev.* **2017**, *79* (April), 984–1001. https://doi.org/10.1016/j.rser.2017.05.164.

(10) Zhang, X.; He, M.; Zhang, Y. A Review of Research on the Kalina Cycle. *Renew.*

Sustain. Energy Rev. **2012**, *16* (7), 5309–5318. https://doi.org/10.1016/j.rser.2012.05.040.

(11) Iqbal, M. A.; Ahmadi, M.; Melhem, F.; Rana, S.; Akbarzadeh, A.; Date, A. Power Generation from Low Grade Heat Using Trilateral Flash Cycle. *Energy Procedia* **2017**, *110* (December 2016), 492–497. https://doi.org/10.1016/j.egypro.2017.03.174.

(12) Monfray, S.; Puscasu, O.; Savelli, G.; Soupremanien, U.; Ollier, E.; Guerin, C.; Fréchette, L. G.; Léveille, E.; Mirshekari, G.; Maitre, C.; Coronel, P.; Domanski, K.; Grabiec, P.; Ancey, P.; Guyomar, D.; Bottarel, V.; Ricotti, G.; Boeuf, F.; Gaillard, F.; Skotnicki, T. Innovative Thermal Energy Harvesting for Zero Power Electronics. *2012 IEEE Silicon Nanoelectron. Work. SNW 2012* **2012**. https://doi.org/10.1109/SNW.2012.6243313.

(13) Covaci, C.; Gontean, A. Piezoelectric Energy Harvesting Solutions: A Review. *Sensors (Switzerland)* **2020**, *20* (12), 1–37. https://doi.org/10.3390/s20123512.

(14) Franco, A.; Filippeschi, S. Closed Loop Two-Phase Thermosyphon of Small Dimensions: A Review of the Experimental Results. *Microgravity Sci. Technol.* **2012**, *24* (3), 165–179. https://doi.org/10.1007/s12217-011-9281-6.

(15) BERGMAN, T. L.; LAVINE, A. S.; INCROPERA, F. P.; DEWITT, D. P. *Fundamentals of Heat and Mass Transfer*, 7th ed.; Ratts, L., Marchione, R., Ruel, C., Sinclair, D., Dumas, S., Lai, W., Kulesa, T., Eds.; John Wiley & Sons, Inc.: New jersy, 2011.

(16) Franco, A.; Filippeschi, S. Experimental Analysis of Heat and Mass Transfer in Small Dimension, Two-Phase Loop Thermosyphons. *Heat Pipe Sci. Technol. An Int. J.* **2010**, *1* (2), 163–182. https://doi.org/10.1615/heatpipescitech.v1.i2.40.

(17) Cole, R.; Shulman, H. L. Bubble Growth Rates at High Jakob Numbers. *Int. J. Heat Mass Transf.* **1966**, *9* (12), 1377–1390. https://doi.org/10.1016/0017-9310(66)90135-9.

(18) Jafari, D.; Franco, A.; Filippeschi, S.; Di Marco, P. Two-Phase Closed Thermosyphons: A Review of Studies and Solar Applications. *Renew. Sustain. Energy Rev.* **2016**, *53*, 575–593. https://doi.org/10.1016/j.rser.2015.09.002.

(19) Kang, J. W.; Diky, V.; Chirico, R. D.; Magee, J. W.; Muzny, C. D.; Abdulagatov, I.; Kazakov, A. F.; Frenkel, M. A New Method for Evaluation of UNIFAC Interaction Parameters. *Fluid Phase Equilib.* **2011**, *309* (1), 68–75.

https://doi.org/10.1016/j.fluid.2011.07.001.

(20) Dr. Michael J. Garbade. Understanding K-means Clustering in Machine Learning https://towardsdatascience.com/understanding-k-means-clustering-in-machine-learning-6a6e67336aa1 (accessed Dec 2, 2020).

(21) university of cincinnati. K-means Cluster Analysis · UC Business Analytics R Programming Guide https://uc-r.github.io/kmeans_clustering (accessed Dec 2, 2020).

(22) Kiatsiriroat, T.; Nuntaphan, A.; Tiansuwan, J. Thermal Performance Enhancement of Thermosyphon Heat Pipe with Binary Working Fluids. *Exp. Heat Transf.* **2000**, *13* (2), 137–152. https://doi.org/10.1080/089161500269517.

(23) Hashimoto, H.; Kaminaga, F. Heat Transfer Characteristics in a Condenser of Closed Two-Phase Thermosyphon: Effect of Entrainment on Heat Transfer Deterioration. *Heat Transf. - Asian Res.* **2002**, *31* (3), 212–225. https://doi.org/10.1002/htj.10030.

(24) Enaburekhan, J.; Yakasai, U. T. Performance Evaluation of a Refrigerant-Charged Integrated Solar Water Heater in Northern Nigeria. *Desalination* **2009**, *243* (1–3), 208–217. https://doi.org/10.1016/j.desal.2008.05.014.

(25) Franco, A. Heat Transfer and Flow Pattern in Two-Phase Loops: An Experimental Investigation. *Proc. 5th Eur. Therm. Sci. ...* **2008**, No. December.

APPENDIX

Appendix A:Pure compound data

Table A-1: Correlation properties of pure compound data at 50°C (part 1).

Chemical Name	h_{fg} (kJ/kmol)	C_p^l (kJ/(kmol*K))	C_p^{ig} (J/(kmol*K))
METHYL-BROMIDE	22219.44	88.09	44.47
METHYL-IODIDE	26998.09	87.43	45.99
METHYLAMINE	21985.06	106.62	55.96
BROMOETHANE	26411.68	105.08	68.04
METHYLACETYLENE	17118.80	115.16	63.89
VINYL-CHLORIDE	18318.91	93.99	56.56
ETHYLAMINE	24999.40	130.10	76.81
ACETALDEHYDE	22133.22	111.91	58.03
ETHYL-MERCAPTAN	25993.22	121.22	76.91
DICHLOROMETHANE	27755.97	104.73	53.50
CARBON-DISULFIDE	26877.59	77.61	46.83
DIMETHYL-SULFIDE	26462.22	121.20	77.56
CYCLOPROPANE	15268.42	100.04	60.84
ISOPROPYL-CHLORIDE	25761.92	138.84	92.83
1,1-DICHLOROETHYLENE	25051.94	115.86	70.06
TRIMETHYLAMINE	20349.73	144.85	97.91
2,2-DIMETHYLBUTANE	26391.88	199.10	151.87
CHLOROPENTAFLUOROETHANE	11559.33	198.56	113.24
OCTAFLUOROPROPANE	11068.56	257.34	154.62
ISOPENTANE	23369.07	175.47	127.89
ISOPRENE	24613.46	162.12	109.91
2-METHYL-1-BUTENE-3-YNE	24134.17	140.41	101.26
1-BUTENE	18637.94	134.62	91.43
1,3-BUTADIENE	19130.96	131.52	85.72
ETHYLACETYLENE	21828.98	138.18	86.41
3-CHLOROPROPENE	28797.86	119.83	79.39
n-PROPYLAMINE	29379.64	164.74	101.42
METHYL-VINYL-ETHER	21605.58	132.62	81.38
METHYL-FORMATE	27057.14	128.59	69.75
1-PENTENE	24127.30	161.23	115.71
METHYLAL	27792.43	167.56	97.29
ETHYL-VINYL-ETHER	26041.20	167.90	104.09
PROPYLENE	11751.50	126.18	68.79
ISOBUTENE	18534.14	138.72	93.79
OCTAFLUOROCYCLOBUTANE	18165.08	214.55	164.15
1-PROPANAL	28484.41	136.70	84.02
1-BUTANAL	32563.57	178.13	108.14

DIMETHYLAMINE	23258.86	128.76	75.17
CYCLOPENTENE	26602.34	131.73	88.96
CYCLOBUTANE	22088.26	119.19	77.27
CYCLOPENTANE	27130.36	136.12	92.37
DECAFLUOROBUTANE	18276.48	265.26	198.95
1,1-DICHLOROTETRAFLUOROETHANE	19914.47	195.73	120.82
NEOPENTANE	20146.87	174.73	130.69
DIMETHYLACETYLENE	25103.38	128.28	81.86
2-METHYL-2-BUTENE	25677.17	160.28	111.81
n-PROPYL-CHLORIDE	27003.43	134.32	90.31
METHYL-ETHYL-ETHER	21329.45	167.33	97.42
CYCLOPENTADIENE	25183.08	135.32	82.65
METHYL-n-PROPYL-ETHER	26066.15	171.80	118.56
2-CHLOROPROPENE	22970.18	125.15	84.21
3,3-DIMETHYL-1-BUTENE	25393.97	200.10	135.00
3-METHYL-1-BUTENE	22413.72	164.78	125.73
2-METHYL-1-BUTENE	24351.08	165.40	116.86
cis-2-BUTENE	20563.36	136.96	85.76
1,4-PENTADIENE	22825.90	154.50	105.42
3-METHYL-1-BUTYNE	24755.50	166.95	110.85
1-PENTYNE	26743.64	169.12	112.76
ETHYL-FLUORIDE	14639.67	123.10	62.98
1,1-DIFLUOROETHANE	16481.63	91.60	72.57
ETHYLENE-OXIDE	23554.39	92.99	51.56
METHYL-MERCAPTAN	22286.19	91.97	52.39
1,2-PROPYLENE-OXIDE	26633.86	126.52	77.81
ISOPROPYLAMINE	26704.55	167.23	103.87
tert-BUTYLAMINE	27248.00	195.75	127.87
cis-2-PENTENE	25561.93	159.36	105.71
trans-2-BUTENE	19734.01	137.09	92.80
DIMETHYL-ETHER	16799.94	113.36	69.32
1,1,1-TRIFLUOROETHANE	10706.50	178.07	83.07
VINYL-BROMIDE	23336.85	109.53	58.33
METHYL-ISOPROPYL-ETHER	25275.76	169.41	117.49
PROPIONITRILE	34570.69	123.03	77.92
ETHYL-PROPYL-ETHER	28975.09	204.60	142.66
Benzene,fluoro-	33279.80	151.01	102.29
CHLORODIFLUOROMETHANE	13449.06	123.33	59.98
METHYL-ISOCYANATE	26202.00	92.89	53.93
cis-1,3-PENTADIENE	26292.85	154.46	103.88
PS: Some data is calculated by ProPrep in ProCAPE			

Table A-2: Correlation properties of pure compound data at 50°C (part 2).

Chemical Name	ρ_l (kmol/m^3)	μ_l (kg/(m*s))	k_l (J/(m*s*K))	σ_l (kg/s^2)
METHYL-BROMIDE	16.75	2.55E-04	9.46E-02	1.73E-02
METHYL-IODIDE	15.44	3.89E-04	8.62E-02	2.57E-02
METHYLAMINE	19.96	1.43E-04	1.61E-01	1.49E-02
BROMOETHANE	12.78	3.01E-04	9.52E-02	1.97E-02
METHYLACETYLENE	14.16	1.20E-04	1.27E-01	8.30E-03
VINYL-CHLORIDE	13.72	1.41E-04	1.12E-01	1.22E-02
ETHYLAMINE	14.29	1.30E-04	1.48E-01	1.54E-02
ACETALDEHYDE	16.79	1.65E-04	1.52E-01	1.70E-02
ETHYL-MERCAPTAN	12.92	2.34E-04	1.57E-01	1.30E-01
DICHLOROMETHANE	14.95	3.34E-04	1.30E-01	2.32E-02
CARBON-DISULFIDE	15.97	3.03E-04	1.44E-01	2.78E-02
DIMETHYL-SULFIDE	13.10	2.30E-04	1.32E-01	2.08E-02
CYCLOPROPANE	13.35	1.34E-04	1.19E-01	8.14E-03
ISOPROPYL-CHLORIDE	10.50	2.44E-04	1.11E-01	1.58E-02
1,1-DICHLOROETHYLENE	11.96	3.01E-04	9.79E-02	2.02E-02
TRIMETHYLAMINE	10.08	1.41E-04	1.21E-01	1.03E-02
2,2-DIMETHYLBUTANE	7.20	2.58E-04	9.48E-02	1.34E-02
CHLOROPENTAFLUOROETHANE	7.38	1.40E-04	4.41E-02	2.27E-03
OCTAFLUOROPROPANE	6.07	2.45E-04	4.09E-02	1.46E-03
ISOPENTANE	8.17	1.92E-04	1.02E-01	1.18E-02
ISOPRENE	9.53	1.67E-04	1.12E-01	1.36E-02
2-METHYL-1-BUTENE-3-YNE	10.16	2.28E-04	1.11E-01	1.46E-02
1-BUTENE	9.86	1.30E-04	1.18E-01	9.12E-03
1,3-BUTADIENE	10.76	1.06E-04	1.22E-01	9.47E-03
ETHYLACETYLENE	11.38	1.71E-04	1.30E-01	1.41E-02
3-CHLOROPROPENE	11.72	2.53E-04	1.18E-01	1.96E-02
n-PROPYLAMINE	11.64	2.84E-04	1.68E-01	1.81E-02
METHYL-VINYL-ETHER	12.19	1.22E-04	1.30E-01	1.31E-02
METHYL-FORMATE	15.47	2.72E-04	1.73E-01	2.02E-02
1-PENTENE	8.65	1.60E-04	1.08E-01	1.28E-02
METHYLAL	10.78	2.62E-04	1.33E-01	1.73E-02
ETHYL-VINYL-ETHER	9.98	1.70E-04	1.28E-01	1.50E-02
PROPYLENE	10.77	8.01E-05	9.01E-02	3.93E-03
ISOBUTENE	9.89	1.66E-04	9.42E-02	8.73E-03
OCTAFLUOROCYCLOBUTANE	6.93	2.80E-04	5.83E-02	5.09E-03
1-PROPANAL	13.11	2.52E-04	1.53E-01	1.86E-02
1-BUTANAL	10.71	3.28E-04	1.39E-01	2.18E-02

DIMETHYLAMINE	13.75	1.56E-04	1.36E-01	1.32E-02
CYCLOPENTENE	10.85	2.61E-04	1.28E-01	1.88E-02
CYCLOBUTANE	11.81	2.19E-04	1.31E-01	1.57E-02
CYCLOPENTANE	10.25	3.22E-04	1.19E-01	1.83E-02
DECAFLUOROBUTANE	5.84	6.68E-04	4.63E-02	4.78E-03
1,1-DICHLOROTETRAFLUOROETHANE	8.05	3.63E-04	6.17E-02	1.11E-02
NEOPENTANE	7.70	1.78E-04	1.12E-01	8.40E-03
DIMETHYLACETYLENE	12.15	1.69E-04	1.15E-01	1.74E-02
2-METHYL-2-BUTENE	8.96	1.69E-04	1.02E-01	1.39E-02
n-PROPYL-CHLORIDE	10.86	2.69E-04	1.10E-01	1.80E-02
METHYL-ETHYL-ETHER	10.97	1.34E-04	1.27E-01	1.19E-02
CYCLOPENTADIENE	11.65	2.43E-04	1.26E-01	1.86E-02
METHYL-n-PROPYL-ETHER	9.41	1.95E-04	1.26E-01	1.48E-02
2-CHLOROPROPENE	11.22	2.55E-04	1.09E-01	1.55E-02
3,3-DIMETHYL-1-BUTENE	7.39	2.09E-04	9.69E-02	1.16E-02
3-METHYL-1-BUTENE	8.46	1.69E-04	1.19E-01	1.12E-02
2-METHYL-1-BUTENE	8.80	1.78E-04	1.01E-01	1.30E-02
cis-2-BUTENE	10.45	1.18E-04	1.25E-01	1.09E-02
1,4-PENTADIENE	9.10	1.67E-04	1.12E-01	1.23E-02
3-METHYL-1-BUTYNE	9.23	2.77E-04	1.03E-01	1.26E-02
1-PENTYNE	9.59	2.83E-04	1.17E-01	1.59E-02
ETHYL-FLUORIDE	13.66	8.71E-05	1.00E-01	5.97E-03
1,1-DIFLUOROETHANE	12.55	1.30E-04	9.39E-02	6.67E-03
ETHYLENE-OXIDE	18.85	1.13E-04	1.48E-01	1.97E-02
METHYL-MERCAPTAN	17.18	2.07E-04	1.40E-01	1.97E-02
1,2-PROPYLENE-OXIDE	13.61	1.60E-04	1.39E-01	1.82E-02
ISOPROPYLAMINE	11.09	2.50E-04	1.13E-01	1.44E-02
tert-BUTYLAMINE	9.07	3.31E-04	1.42E-01	1.44E-02
cis-2-PENTENE	8.86	1.79E-04	1.10E-01	1.39E-02
trans-2-BUTENE	10.12	1.18E-04	1.24E-01	1.05E-02
DIMETHYL-ETHER	13.29	9.38E-05	1.30E-01	8.04E-03
1,1,1-TRIFLUOROETHANE	9.94	9.25E-05	5.90E-02	2.47E-03
VINYL-BROMIDE	13.56	2.96E-04	9.13E-02	1.58E-02
METHYL-ISOPROPYL-ETHER	9.27	1.48E-04	1.20E-01	1.28E-02
PROPIONITRILE	13.67	3.19E-04	1.59E-01	2.38E-02
ETHYL-PROPYL-ETHER	7.90	2.36E-04	1.21E-01	1.66E-02
Benzene,fluoro-	10.30	4.18E-04	1.19E-01	2.35E-02
CHLORODIFLUOROMETHANE	12.51	1.55E-04	7.47E-02	4.73E-03
METHYL-ISOCYANATE	15.58		1.24E-01	2.20E-02
cis-1,3-PENTADIENE	9.69	1.67E-04	1.17E-01	1.54E-02
PS: Some data is calculated by ProPrep in ProCAPE				

Table A-3: Safety of pure compound data.

Chemical name	Cas-no	NFPA: B	NFPA: R	NFPA: Y
DIETHYL-ETHER	000060-29-7	2	4	1
ETHANOL	000064-17-5	1	3	0
METHANOL	000067-56-1	2	3	0
ISOPROPANOL	000067-63-0	2	3	1
ACETONE	000067-64-1	2	3	0
CHLOROFORM	000067-66-3	2	0	0
1-PROPANOL	000071-23-8	2	3	0
METHYL-BROMIDE	000074-83-9	3	1	0
METHYL-IODIDE	000074-88-4	4	0	1
METHYLAMINE	000074-89-5	3	4	0
DIBROMOMETHANE	000074-95-3	3	0	0
BROMOETHANE	000074-96-4	3	3	0
BROMOCHLOROMETHANE	000074-97-5	2	0	0
PROPANE	000074-98-6	2	4	0
METHYLACETYLENE	000074-99-7	2	4	3
ETHYL-CHLORIDE	000075-00-3	2	4	0
VINYL-CHLORIDE	000075-01-4	2	4	2
ETHYLAMINE	000075-04-7	3	4	0
ACETONITRILE	000075-05-8	2	3	1
ACETALDEHYDE	000075-07-0	2	4	2
ETHYL-MERCAPTAN	000075-08-1	1	4	1
DICHLOROMETHANE	000075-09-2	2	0	0
CARBON-DISULFIDE	000075-15-0	2	3	0
DIMETHYL-SULFIDE	000075-18-3	2	4	0
CYCLOPROPANE	000075-19-4	1	4	0
2-BROMOPROPANE	000075-26-3	2	3	0
ISOBUTANE	000075-28-5	2	4	0
ISOPROPYL-CHLORIDE	000075-29-6	2	4	0
1,1-DICHLOROETHANE	000075-34-3	2	3	0
1,1-DICHLOROETHYLENE	000075-35-4	1	3	0
DICHLOROFLUOROMETHANE	000075-43-4	1	0	1
TRIMETHYLAMINE	000075-50-3	3	4	0
1-CHLORO-1,1-DIFLUOROETHANE	000075-68-3	2	3	0
TRICHLOROFLUOROMETHANE	000075-69-4	2	0	0
DICHLORODIFLUOROMETHANE	000075-71-8	1	0	0
2,2-DIMETHYLBUTANE	000075-83-2	2	4	0
1,1,2-TRICHLOROTRIFLUOROETHANE	000076-13-1	2	1	0
CHLOROPENTAFLUOROETHANE	000076-15-3	3	0	0
OCTAFLUOROPROPANE	000076-19-7	1	0	0
ISOPENTANE	000078-78-4	2	4	0
ISOPRENE	000078-79-5	0	4	0

2-METHYL-1-BUTENE-3-YNE	000078-80-8	2	4	2
ISOBUTYLAMINE	000078-81-9	3	4	0
2-METHYLPROPANAL	000078-84-2	2	3	1
METHACROLEIN	000078-85-3	3	3	2
sec-BUTYL-CHLORIDE	000078-86-4	2	4	0
1,2-DICHLOROPROPANE	000078-87-5	3	4	0
2-BUTANOL	000078-92-2	1	3	0
METHYL-ETHYL-KETONE	000078-93-3	3	3	0
DICHLOROACETALDEHYDE	000079-02-7	1	2	0
METHYL-ACETATE	000079-20-9	1	3	0
2,3-DIMETHYLBUTANE	000079-29-8	2	3	0
3-METHYLPENTANE	000096-14-0	2	4	0
METHYLCYCLOPENTANE	000096-37-7	2	3	0
1,2-EPOXYBUTANE	000106-88-7	2	3	2
n-BUTANE	000106-97-8	1	4	0
1-BUTENE	000106-98-9	1	4	0
1,3-BUTADIENE	000106-99-0	2	4	2
ETHYLACETYLENE	000107-00-6	0	4	0
ACROLEIN	000107-02-8	4	3	3
3-CHLOROPROPENE	000107-05-1	3	3	1
1,2-DICHLOROETHANE	000107-06-2	2	3	0
n-PROPYLAMINE	000107-10-8	3	3	0
ALLYLAMINE	000107-11-9	4	0	0
ALLYL-ALCOHOL	000107-18-6	3	0	0
GLYOXAL	000107-22-2	1	2	0
METHYL-VINYL-ETHER	000107-25-5	0	4	2
METHYL-FORMATE	000107-31-3	2	4	0
VINYL-ACETATE	000108-05-4	2	4	2
2,4-DIMETHYLPENTANE	000108-08-7	2	3	0
DIISOPROPYLAMINE	000108-18-9	3	3	0
DIISOPROPYL-ETHER	000108-20-3	2	4	1
n-PENTANE	000109-66-0	1	4	0
1-PENTENE	000109-67-1	2	4	0
METHYLAL	000109-87-5	2	3	2
DIETHYLAMINE	000109-89-7	3	4	0
ETHYL-VINYL-ETHER	000109-92-2	2	4	2
ETHYL-FORMATE	000109-94-4	3	4	1
n-HEXANE	000110-54-3	2	3	0
1,2-DIMETHOXYETHANE	000110-71-4	1	4	1
n-PROPYL-FORMATE	000110-74-7	2	3	0
PROPYLENE	000115-07-1	1	4	1
ISOBUTENE	000115-11-7	1	4	0
OCTAFLUOROCYCLOBUTANE	000115-25-3	1	0	0
1-PROPANAL	000123-38-6	2	3	1

1-BUTANAL	000123-72-8	3	3	0
DIMETHYLAMINE	000124-40-3	3	4	0
CHLOROPRENE	000126-99-8	2	3	3
ETHYL-ACETATE	000141-78-6	1	3	0
CYCLOPENTENE	000142-29-0	2	4	0
cis-1,2-DICHLOROETHYLENE	000156-59-2	1	3	2
CYCLOBUTANE	000287-23-0	1	4	0
CYCLOPENTANE	000287-92-3	1	3	0
DECAFLUOROBUTANE	000355-25-9	1	0	0
NEOPENTANE	000463-82-1	0	4	0
DIMETHYLACETYLENE	000503-17-3	1	4	0
tert-BUTYL-CHLORIDE	000507-20-0	2	3	0
2-METHYL-2-BUTENE	000513-35-9	2	4	0
n-PROPYL-CHLORIDE	000540-54-5	2	3	0
METHYL-ETHYL-ETHER	000540-67-0	2	4	1
METHYL-n-PROPYL-ETHER	000557-17-5	2	3	0
2-CHLOROPROPENE	000557-98-2	2	4	0
3,3-DIMETHYL-1-BUTENE	000558-37-2	2	3	0
3-METHYL-1-BUTENE	000563-45-1	2	4	0
2-METHYL-1-BUTENE	000563-46-2	1	4	0
cis-2-BUTENE	000590-18-1	1	4	0
1,4-PENTADIENE	000591-93-5	2	4	0
3-METHYL-1-BUTYNE	000598-23-2	1	4	0
1-PENTYNE	000627-19-0	1	3	0
cis-2-PENTENE	000627-20-3	2	4	0
trans-2-BUTENE	000624-64-6	1	4	0
4-METHYL-1-PENTENE	000691-37-2	2	4	0
DIMETHYL-ETHER	000115-10-6	2	4	1
1,1,1-TRIFLUOROETHANE	000420-46-2	3	3	0
VINYL-BROMIDE	000593-60-2	3	4	0
2,2,3-TRIMETHYLBUTANE	000464-06-2	2	3	0
4-METHYL-cis-2-PENTENE	000691-38-3	2	4	0
PROPIONITRILE	000107-12-0	3	4	0
2,3-DIMETHYL-1-BUTENE	000563-78-0	1	4	0
1,5-HEXADIENE	000592-42-7	2	3	2
TETRAHYDROFURAN	000109-99-9	2	3	1
ETHYL-PROPYL-ETHER	000628-32-0	1	3	0
2,3-DIMETHYL-2-BUTENE	000563-79-1	1	4	0
2-METHYL-2-PENTENE	000625-27-4	2	4	0
tert-BUTYL-ETHYL-ETHER	000637-92-3	2	3	0
trans-1,2-DIMETHYLCYCLOPENTANE	000822-50-4	0	3	0
CYCLOHEXANE	000110-82-7	1	3	0
CYCLOHEXENE	000110-83-8	1	3	1
N-METHYLPYRROLIDINE	000120-94-5	1	4	0

2,3-DIMETHYL-1,3-BUTADIENE	000513-81-5	1	4	0
1-HEXENE	000592-41-6	2	4	0
1,4-HEXADIENE	000592-45-0	2	4	0
1,3-CYCLOHEXADIENE	000592-57-4	1	3	0
1-METHYLCYCLOPENTENE	000693-89-0	1	3	1
2-ETHYL-1-BUTENE	000760-21-4	2	4	0
HEXAFLUOROBENZENE	000392-56-3	1	3	1
Benzene,fluoro-	000462-06-6	1	4	0
PENTAFLUOROETHANE	000354-33-6	2	0	0
ETHYL-FLUORIDE	000353-36-6	0	3	0
1,1-DIFLUOROETHANE	000075-37-6	2	4	0
ETHYLENE-OXIDE	000075-21-8	3	4	3
METHYL-MERCAPTAN	000074-93-1	4	4	1
n-HEPTANE	000142-82-5	1	3	0
1,2-PROPYLENE-OXIDE	000075-56-9	3	4	0
ISOPROPYLAMINE	000075-31-0	3	4	0
ISOPROPYL-MERCAPTAN	000075-33-2	2	3	0
CHLOROMETHYL-METHYL-ETHER	000107-30-2	2	3	0
ACRYLONITRILE	000107-13-1	4	3	2
tert-BUTYLAMINE	000075-64-9	3	4	0
tert-BUTYL-MERCAPTAN	000075-66-1	2	4	0
1,1,1,2-TETRAFLUOROETHANE	000811-97-2	1	0	1
CHLORODIFLUOROMETHANE	000075-45-6	2	0	0
cis-1,3-PENTADIENE	001574-41-0	2	3	2
1,2-DICHLORO-1,1,2-TRIFLUOROETHANE	000354-23-4	3	0	0
1,1-DICHLORO-1-FLUOROETHANE	001717-00-6	1	3	0
WATER	007732-18-5	0	0	0
4-METHYL-trans-2-PENTENE	000674-76-0	1	3	0
Data source: pubchem.ncbi.nlm.nih.gov				

Appendix B:Result of data mining

Appendix B-1:Statistic values of database.

Table B-2: Statistic values of primary properties database.

properties	unit	Mean values	Standard deviation	Minimum values	Maximum values
ρ_l	[kmol/m3]	11.044	2.561	5.867	30.029
ρ_v	[kmol/m3]	0.139	0.167	0.038	1.444
k_l	[J/m·s·K]	0.116	0.028	0.043	0.359
μ_l	[kg/ms]	2.34E-04	9.50E-05	7.57E-05	6.67E-04
σ_l	[kg/s^2]	1.45E-02	4.92E-03	1.61E-03	2.78E-02
C_p^l	$\left[\frac{kJ}{kmolK}\right]$	148.828	31.022	77.923	264.571
h_{fg}	[kJ/kmol]	2.41E+04	4.00E+03	1.06E+04	3.57E+04
C_p^{ig}	$\left[\frac{kJ}{kmolK}\right]$	98.238	26.26	44.507	198.367

Table B-3: Statistic values of secondaries properties database.

properties	Mean values	Standard deviation	Minimum values	Maximum values
Bo_{cal}	7.22E+04	7.71E+04	2.94E+04	6.15E+05
Ja_{ig}^{cal}	4.27E-03	1.72E-03	1.56E-03	1.33E-02
Ja_l^{cal}	6.48E-03	2.46E-03	2.70E-03	2.19E-02
h_c^{cal}	7.07E+02	1.55E+02	2.91E+02	1.57E+03
h_e^{cal}	1.67E+04	2.69E+04	3.45E+03	2.30E+05
X_{cal}	9.34E+05	2.34E+06	6.22E+04	1.90E+07
Notice: The values in this table are calculated from equation in appendix C-1.				

Table B-4: Statistic values of safety database (NFPA 704).

NFPA 704	Mean values	Standard deviation	Minimum values	Maximum values
B_1	1.936	0.825	0	4
B_2	1.519	0.777	0	4
R_1	3.157	1.245	0	4
R_2	3.323	1.151	0	4
Y_1	0.518	0.827	0	3
Y_2	0.301	0.676	0	3

Appendix B-2:Centroid point of each cluster

Table B-5: Centroid point of each cluster for primaries properties.

Cluster / Properties	0	1	2	3	4	5
ρ_l	0.1679	-0.6526	-1.6458	-0.746	0.3367	1.8352
ρ_v	0.6015	-0.4193	0.688	3.4135	-0.4081	-0.2257
k_l	0.0137	-0.1798	-1.7674	-1.7548	0.385	0.9967
μ_l	-0.9626	-0.1747	3.0688	-0.624	0.2446	0.2065
σ_l	-0.7957	-0.0734	-1.8349	-2.214	0.652	1.1889
C_p^l	-0.4753	0.5468	2.6156	0.8089	-0.4691	-1.2408
h_{fg}	-1.0851	0.3619	-1.2137	-2.618	0.5893	0.3458
C_p^{ig}	-0.4702	0.6076	2.7978	0.2792	-0.4422	-1.3192
Notice: The values were normalized with equation 3.1						

Table B-6: Centroid point of each cluster for secondaries properties.

Cluster / Properties	0	1	2	3
Bo_{cal}	-0.3055	4.6814	1.7265	-0.2559
Ja_{ig}^{cal}	-0.6095	3.2675	2.0257	0.1118
Ja_{l}^{cal}	-0.5405	3.9545	1.8693	0.0195
h_c^{cal}	0.7477	-1.9401	-1.5799	-0.4187
h_e^{cal}	-0.2483	5.1624	0.8732	-0.2071
X_{cal}	-0.2596	5.3559	0.6823	-0.1758
Notice: The values were normalized with equation 3.1				

Table B-7: Centroid point of each cluster for safety database (NFPA 704).

NFPA 704 / Cluster	B_1	B_2	R_1	R_2	Y_1	Y_2
0	-0.0212	-0.9773	0.2595	0.2468	-0.4163	-0.4222
1	0.0560	0.8041	0.2597	0.3349	-0.3007	-0.3520
2	-0.2316	0.3565	0.4562	0.2335	-0.2806	2.3461
3	0.0396	-0.0702	0.4435	0.3145	1.9626	-0.2935
4	-0.4107	0.0469	0.3428	-2.8144	-0.4916	-0.1573
5	0.4097	-0.1805	-2.4682	0.1766	-0.3969	-0.2114
Notice: The values were normalized with equation 3.1						

Appendix C:Equation and calculation

Appendix C-1: Equation for calculation secondaries properties

Bond number (Bo)

$$Bo=\frac{g(\rho_l-\rho_v)d_i^2}{\sigma} \quad 2.1$$

From equation 3.1

$$Bo_{norm}=\frac{Bo-Bo_{mean}}{Bo_{std}} \quad 3.1$$

$$Bo_{norm}=\frac{Bo-Bo_{mean}}{\sqrt{\frac{\sum(Bo-Bo_{mean})^2}{n-1}}} \quad C.1$$

From equation 2.1

$$Bo_{norm}=\frac{gd_i^2\left(\frac{(\rho_l-\rho_v)}{\sigma}-\frac{(\rho_l-\rho_v)}{\sigma}_{mean}\right)}{gd_i^2\sqrt{\frac{\sum\left(\frac{(\rho_l-\rho_v)}{\sigma}-\frac{(\rho_l-\rho_v)}{\sigma}_{mean}\right)^2}{n-1}}} \quad C.2$$

$$Bo_{norm}=\frac{\left(\frac{(\rho_l-\rho_v)}{\sigma}-\frac{(\rho_l-\rho_v)}{\sigma}_{mean}\right)}{\sqrt{\frac{\sum\left(\frac{(\rho_l-\rho_v)}{\sigma}-\frac{(\rho_l-\rho_v)}{\sigma}_{mean}\right)^2}{n-1}}} \quad C.3$$

Due to calculation normalization use properties only ρ_l , ρ_v and σ. Therefore, Bo for calculation is

$$Bo_{cal}=\frac{(\rho_l-\rho_v)}{\sigma} \quad C.4$$

Jakob number (Ja)

$$Ja=\frac{C_p(T_s-T_{sat})}{h_{fg}} \quad 2.5$$

Assumption $T_s-T_{sat}=1$. Therefore, Ja for calculation is

$$Ja_{cal}=\frac{C_p}{h_{fg}} \quad C.5$$

heat transfer coefficient for condenser (h_c)

$$h_c=0.85Re_f^{0.1}\exp\left(-0.000067\frac{\rho_l}{\rho_v}-0.6\right)h_{c,Nust} \quad 2.1$$

Where,

$$h_{c,Nust}=0.943\left\{\frac{\rho_l g k_l^3(\rho_l-\rho_v)[h_{fg}+0.68C_{pl}(T_{sat}-T_s)]}{\mu_l(T_{sat}-T_s)L_c}\right\}^{1/4} \quad 2.2$$

$$Re_f=\frac{4Q}{\pi d h_{fg}\mu_l} \quad 2.8$$

Thus,

$$h_c=0.801\left(\frac{4Q}{\pi d h_{fg}\mu_l}\right)^{0.1}\exp\left(-0.000067\frac{\rho_l}{\rho_v}-0.6\right)\left\{\frac{\rho_l g k_l^3(\rho_l-\rho_v)[h_{fg}+0.68C_{pl}(T_{sat}-T_s)]}{\mu_l(T_{sat}-T_s)L_c}\right\}^{1/4} \quad C.6$$

$$h_c=\frac{0.453g^{1/4}}{d_i^{0.1}L_c^{1/4}}\left(\frac{Q}{h_{fg}\mu_l}\right)^{0.1}\exp\left(-0.000067\frac{\rho_l}{\rho_v}\right)\left\{\frac{\rho_l k_l^3(\rho_l-\rho_v)[h_{fg}+0.68C_{pl}(T_{sat}-T_s)]}{\mu_l(T_{sat}-T_s)}\right\}^{1/4} \quad C.7$$

Assumption T_s-T_{sat} = 1 and Q constant. Thus,

$$h_c=\frac{0.453g^{1/4}Q^{0.1}}{d_i^{0.1}L_c^{1/4}}\exp\left(-0.000067\frac{\rho_l}{\rho_v}\right)\frac{[\rho_l k_l^3(\rho_l-\rho_v)(h_{fg}+0.68C_{pl})]^{1/4}}{\mu_l^{0.35}h_{fg}^{0.1}} \quad C.8$$

Due to normalization can eliminate constant values which is solved in equation C.2 to C.3. Thus, h_c for calculation is

$$h_c^{cal}=\exp\left(-0.000067\frac{\rho_l}{\rho_v}\right)\frac{[\rho_l k_l^3(\rho_l-\rho_v)(h_{fg}+0.68C_{pl})]^{1/4}}{\mu_l^{0.35}h_{fg}^{0.1}} \quad C.9$$

heat transfer coefficient for evaporator (h_e)

Because h_e has many equations to calculate, so nucleate boiling case is chosen. Due to, this case gives the highest value of h_e and make more different to compare with other compounds.

For nu nucleate boiling, he is

$$h_e=6.95\times10^{-4}(1+4.95\Psi)\frac{k_l}{L_b}\left(\frac{qPL_b^2}{\rho_v h_{fg}\nu_l\sigma}\right)^{0.7}Pr_l^{0.35} \quad 2.14$$

Where,

$$L_b=\sqrt{\frac{\sigma}{g(\rho_l-\rho_v)}} \quad 2.4$$

Thus,

$$h_e=6.95\times10^{-4}(1+4.95\Psi)\frac{k_l}{\sqrt{\frac{\sigma}{g(\rho_l-\rho_v)}}}\left(\frac{qP\frac{\sigma}{g(\rho_l-\rho_v)}}{\rho_v h_{fg}\nu_l\sigma}\right)^{0.7}Pr_l^{0.35} \quad C.10$$

Assumption Q constant. Thus,

$$h_e=\frac{6.95\times10^{-4}g^{0.5}}{(gq)^{0.7}}(1+4.95\Psi)\frac{k_l}{\sqrt{\frac{\sigma}{(\rho_l-\rho_v)}}}\left(\frac{P\frac{\sigma}{(\rho_l-\rho_v)}}{\rho_v h_{fg}\nu_l\sigma}\right)^{0.7}Pr_l^{0.35} \quad C.11$$

Due to normalization can eliminate constant values which is solved in equation C.2 to C.3. Thus, h_e for calculation is

$$h_e^{cal}=(1+4.95\Psi)\frac{k_l}{\sqrt{\frac{\sigma}{(\rho_l-\rho_v)}}}\left(\frac{P\frac{\sigma}{(\rho_l-\rho_v)}}{\rho_v h_{fg}\nu_l\sigma}\right)^{0.7}Pr_l^{0.35} \quad C.12$$

dimensionless pool parameter (X)

$$X=\Psi(RaPr_l)^{0.35}\left(\frac{P_vL_b^2q}{\sigma\rho_vh_{fg}\nu_l}\right)^{0.7} \quad 2.9$$

where,

$$\Psi=\left(\frac{\rho_v}{\rho_l}\right)^{0.4}\left[\frac{P_v\nu_l}{\sigma}\left(\frac{\rho_l^2}{\sigma g(\rho_l-\rho_v)}\right)^{1/4}\right]^{1/4} \quad 2.10$$

Thus,

$$X=\left(\frac{\rho_v}{\rho_l}\right)^{0.4}\left[\frac{P_v\nu_l}{\sigma}\left(\frac{\rho_l^2}{\sigma g(\rho_l-\rho_v)}\right)^{1/4}\right]^{1/4}\left(\frac{\Delta\,\rho_lL_c^3g\,\rho_lC_p^l}{\mu_lk}Pr_l\right)^{0.35}\left(\frac{P_vL_b^2q}{\sigma\rho_vh_{fg}\nu_l}\right)^{0.7} \quad C.13$$

Assumption Q constant. Thus,

$$X=\left(\frac{q^2L_c^3}{g}\right)^{0.35}\left(\frac{\rho_v}{\rho_l}\right)^{0.4}\left[\frac{P_v\nu_l}{\sigma}\left(\frac{\rho_l^2}{\sigma g(\rho_l-\rho_v)}\right)^{1/4}\right]^{1/4}\left(\frac{\Delta\,\rho_lL_c^3g\,\rho_lC_p^l}{\mu_lk}Pr_l\right)^{0.35}\left(\frac{P_vL_b^2q}{\sigma\rho_vh_{fg}\nu_l}\right)^{0.7} \quad C.14$$

Due to normalization can eliminate constant values which is solved in equation C.2 to C.3. Thus, X for calculation is

$$X_{cal}=\left(\frac{\rho_v}{\rho_l}\right)^{0.4}\left[\frac{P_v\nu_l}{\sigma}\left(\frac{\rho_l^2}{\sigma g(\rho_l-\rho_v)}\right)^{1/4}\right]^{1/4}\left(\frac{\Delta\,\rho_lL_c^3g\,\rho_lC_p^l}{\mu_lk}Pr_l\right)^{0.35}\left(\frac{P_vL_b^2q}{\sigma\rho_vh_{fg}\nu_l}\right)^{0.7} \quad C.15$$

Appendix C-2:K-mean clustering calculation example (R-134a primary properties).

Clustering of K-mean use distance between data point with centroid point as a criterion which is calculated by equation C.16.

$$\text{Distance} = \sqrt{\sum\left(D_{prop}-D_{cen}\right)^2} \quad C.16$$

For primary properties, required properties of R-134 is below.

ρ_l 50°C [kmol/m^3]	10.79
ρ_v 50°C [kmol/m^3]	2.05
k_l 50°C [J/(m·s·K)]	7.06×10^{-2}
μ_l 50°C [kg/(m·s)]	5.03×10^{-3}
σ_l 50°C [kg/s^2]	1.62×10^{-4}
C_p^l 50°C [kJ/(kmol·K]	162.11
h_{fg} 50°C [kJ/kmol]	1.57×10^{4}
C_p^{ig} 50°C [kJ/(kmol·K)]	91.32

And, the centroid point of each cluster is in table B-5. However, the data are normalized by equation 3.1. calculation of normalization is below. The calculation example is below which use data in table B-1.

For normalization of liquid density.

$$\rho_{l,norm} = \frac{10.79-11.042}{2.561} = -0.099 \qquad \text{C.17}$$

All normalized data is show below,

$\rho_{l,norm}$ =	-0.099
$\rho_{v,norm}$ =	11.449
$k_{l,norm}$ =	-1.655
$\mu_{l,norm}$ =	-0.759
$\sigma_{l,norm}$ =	-1.935
$C^{l}_{p,norm}$ =	0.428
$h_{fg,norm}$	-2.095
$C^{ig}_{p,norm}$ =	-0.263

For cluster 0, the distance calculation is below.

$$\begin{aligned} \text{Distance}^2 = {} & (-0.099-0.1679)^2+(11.449-0.6015)^2+(-1.655-0.0137)^2+ \\ & (-0.759-(-0.9626))^2+(-1.935-(-0.7957))^2+ (0.428-(-0.4753))^2+ \\ & (-2.095-(-1.0851))^2+(-0.263-(-0.4702))^2 \\ = {} & 123.748 \end{aligned} \qquad \text{C.18}$$

$$\text{Distance} = \sqrt{123.748} = 11.124 \qquad \text{C.19}$$

Distances of other clusters are below.

Cluster 0	11.124
Cluster 1	12.408
Cluster 2	12.158
Cluster 3	8.112
Cluster 4	12.676
Cluster 5	12.947

Therefore, primary properties cluster of R-134a is cluster 3 because distance between data point with the centroid point is lowest.

BIBLIOGRAHPY

Name: Natchanon Ornsila

Date of Birth: 19/09/1998

Address: 159/381 Soi Khu Bon 27, Khu Bon Road, Tha Raeng, Bang Khen, Bangkok, Thailand 10220

E-mail: NatchanonTaku@gmail.com, 60010297@kmitl.ac.th

Academic Background: Degree of Bachelor of Engineering
Department of Chemical Engineering, Faculty of Engineering
King Mongkut's Institute of Technology Ladkrabang

Working Experience: PSE for SPEED Company Limited